ISTANBUL TECHNICAL UNIVERSITY ★ INSTITUTE OF SCIENCE AND TECHNOLOGY

DESIGN OF A REFRIGERATOR CABINET BASED ON SOLIDIFICATION PROCESS OF POLYURETHANE FOAM FLOW

M.Sc. THESIS

Hamed PAHLAVANI

Department of Mechanical Engineering

Construction Program

May 2015

ISTANBUL TECHNICAL UNIVERSITY ★ INSTITUTE OF SCIENCE AND TECHNOLOGY

DESIGN OF A REFRIGERATOR CABINET BASED ON SOLIDIFICATION PROCESS OF POLYURETHANE FOAM FLOW

M.Sc. THESIS

Hamed PAHLAVANI
(503121224)

Department of Mechanical Engineering

Construction Program

Thesis Advisor: Prof. Dr. İ. Bedii ÖZDEMİR

May 2015

İSTANBUL TEKNİK ÜNİVERSİTESİ ★ FEN BİLİMLERİ ENSTİTÜSÜ

KATILAŞMA SÜRECİ OLAN POLİÜRETAN KÖPÜK AKIŞNA GÜRE YENİ BİR BUZDOLABI KABİNİ TASARIMI

YÜKSEK LİSANS TEZİ

Hamed PAHLAVANI
(503121224)

Makine Mühendisliği Anabilim Dalı

Konstrüksiyon Programı

Tez Danışmanı: Prof. Dr. İ. Bedii ÖZDEMİR

25 May 2015

Hamed PAHLAVANI, a M.Sc. student of ITU Institute of Science and Technology 503121224 successfully defended the thesis entitled **"DESIGN OF A REFRIGERATOR CABINET BASED ON SOLIDIFICATION PROCESS OF POLYURETHANE FOAM FLOW"**, which he/she prepared after fulfilling the requirements specified in the associated legislations, before the jury whose signatures are below.

Thesis Advisor :	**Prof. Dr. İ. Bedii ÖZDEMİR** Istanbul Technical University	.....
Jury Members :	**Assist. Prof. Dr. Berna ALPAN BOLAT** Yıldız Technical University	.....
	Lecturer Dr. Orhan ATABAY Istanbul Technical University	.....

Date of Submission : **04 May 2015**
Date of Defense : **28 May 2015**

To my dear family,

FOREWORD

I would like to express my gratitude to the numerous people who helped me make this work. First of all, I would like to thank my supervisor, Prof. Dr. İ. Bedii ÖZDEMİR for his encouragement and guidence during the preparation of this thesis.

I am also grateful to my officemates, it was a pleasure to work and share knowledge with them.

I would also like to thank SAN-TEZ, for the scholarship that helped me focus on my education.

Finally, I would like to thank my parents, for their endless support and faith in me whenever I had difficult times.

May 2015

Hamed PAHLAVANI
(Mechanical Engineer)

TABLE OF CONTENTS

Page

ABBREVIATIONS

CFD	**:** Computational Fluid Dynamics
PDE	**:** Partial Differential Equation
FDM	**:** Finite Different Method
FVM	**:** Finite Volume Method
FEM	**:** Finite Element Method
URANS	**:** Unsteady Reynolds Averaged Navier-Stokes
N-S	**:** Navier-Stokes
MDI	**:** Methylene Diphenyl diisocyanate
TDI	**:** Toluene Diisocyanate
HDI	**:** Hexamethylene Diisocyanate
IPDI	**:** Isophorone Diisocyanate
PBA	**:** Physicbinal Blowing Agent
UDF	**:** User Defined Functions
App	**:** Appendix

LIST OF TABLES

Page

LIST OF FIGURES

Page

LIST OF SYMBOLS

α	:	Thermal diffusivity
δ_{ij}	:	Kronecker delta
η	:	Length micro scale
$\forall$	:	Volume
Γ_ϕ	:	Diffusion coefficient for ϕ
λ	:	Thermal conductivity
$\mathbf{A_f}$	:	Surface area vector
$\mathbf{F_{visc}}$	:	Viscous force
$\mathbf{n}$	:	Normal vector
$\mathbf{r}$	:	Displacement vector
$\mathbf{x}'$	:	Integration variable
$\mathscr{L}_{ij}$	:	Leonard stress
$\mathscr{P}$	:	Production of turbulence
$\mathscr{T}_{\mathrm{ij}}$	:	Test filtered stress
$\mathscr{T}$	:	Time micro scale
$\mid \widetilde{S} \mid$	:	Magnitude of rate of strain tensor
μ	:	Dynamic viscosity
μ_t	:	Turbulent dynamic viscosity
∇	:	Gradient operator
ν	:	Kinematic viscosity
ϕ	:	Arbitrary scalar
ϕ_f	:	The value of ϕ on the face
ρ	:	Density
σ_{ij}	:	Stress tensor
σ_k	:	Prandtl number for turbulence kinetic energy
τ_{ij}	:	Shear stress tensor
τ_w	:	Wall shear stress
$\tilde{\phi}_f$	:	Average of the values at the cell centroids on the two sides of the face
$\triangle$	:	Filter width
ε	:	Turbulence energy dissipation rate
C	:	Sub-grid scale coefficient
C_μ	:	Empirical constant for y^+
$C_{\varepsilon 1}$	:	Model constant for $k-\varepsilon$
$C_{\varepsilon 2}$	:	Model constant for $k-\varepsilon$
C_I	:	Sub-grid scale coefficient
c_p	:	Specific heat capacity
f	:	Arbitrary vector
G	:	Filtering function
h	:	Enthalpy
I	:	Turbulence intensity

k	:	Turbulent kinetic energy
k_p	:	Turbulent kinetic energy at point p
L	:	Length macro scale
L_m	:	Mean flow characteristic length
p	:	Pressure
Re	:	Reynolds number
Re_L	:	Macro scale Reynolds number
S	:	Area
S_ϕ	:	Source term for ϕ
S_h	:	Viscous dissipation
S_{ij}	:	Rate of strain tensor
T	:	Time macro scale
t	:	Time
u	:	Velocity
u_τ	:	Friction velocity
V_L	:	Macro scale velocity
V_m	:	Mean flow velocity
v_d	:	Fluid domain
y^+	:	Dimensionless wall distance
y^*	:	Wall unit
y_p	:	Distance of point p from wall

DESIGN OF A REFRIGERATOR CABINET BASED ON SOLIDIFICATION PROCESS OF POLYURETHANE FOAM FLOW

SUMMARY

There are many advantages of using polyurethane materials, including low cost, light weight, enhanced thermal and electrical insulation, and high impact strength and, therefore, it has many applications, as for example, producing various kinds of complex parts including automobile interior furnitures, household appliances and housing industry. Use of polyurethane foam is also spreading rapidly in refrigerators as insulation material.

Reaction injection molding of polyurethane foam is a process in that two or more chemical components mix, chemically react and finally form a foam which flows into the mold cavity where the polymerization is initiated. Energy efficiency of modern refrigerators demands a very effective insulation and, hence, the foam is required to fill complex cavities in very short time scales. In order to increase cavity filling efficiency while shorten the injection molding process, it is necessary to understand the phenomena of mixing, reaction kinetics, bubble nucleation and growth and two-phase flow behaviour during mold filling. Lack of control on reactive injection molding parameters results in variations from load to load and even from part to part, leading to serious quality degradation and, thus, the whole process becomes labor-intesive at elevated material costs.International competition between companies is rapidly growing. Hence companies race in the energy efficiency field and invest large amount of money on R&D activities for having more efficient products. For refrigerators; energy efficiency is highly relative to its insulation performance. Rigid polyurethane foam is used as insulation material between the refrigerators cabinet walls. Good insulation performance depends on the homogeneity of foam in the cabinet. Another function of the foam is the mechanical support to thin cabinet walls. Short injection time and minimized chemical costs are desired in mass production. To provide these requirements air outlets orientation, numbers, diameters and progress of chemical reactions, the temperature of the injected mixture and cabinet temperature are important parameters. If we want to find these optimum parameters we have to understand the nature of the polyurethane injection process. Thus polyurethane injection process become more controllable and we can predict process parameters for new designs before the manufacturing. In the light of these informations the aims of the thesis obtained as;

•Decreasing the usage of the foaming materials for single cabinet volume

•Decreasing the costs due to change of the initial conditions of the process,

•Decreasing the foam filling time of the cabinet,

•Increasing the insulation and structural strength performance of the foam with minimizing the air traps in it,

•Optimization positions, sizes and the numbers of air outlets to make the polyurethane injection procces more efficient,

•Understanding the nature of polyurethane flow and getting a solid scientific knowledge about it.

From this point of view a project started by ARCELIK Inc. and ITU Fluids Group with the support of the Ministry of Science Industry and Technology Commissary. A refrigerator with two doors chosen for the computational fluid dynamics (CFD) simulations. Flow of the rigid polyurethane foam in the cabinet is three dimensional, reactive, multiphase and time dependent. Also solidification occurs due to chemical reactions. Chemical reactions effect the flow very strongly. Except the CFD simulations, a chemical kinetics study has been done without flow to obtain optimum initial reaction conditions locally such as initial mass fractions of the species and initial temperature. ANSYS Meshing and ICEM CFD were used for mesh generation. CATIA and SOLIDWORKS were used for CAD and geometry refinements. On the other hand a FORTRAN code were used for modeling the chemical kinetics. Chemistry code was developed in the ITU Fluids Group. CFD simulations were done with the FLUENT software. Chemistry code was implemented in FLUENT by using the user defined functions (UDF) and they run simultaneously. Post processing had been done with the TECPLOT and MATLAB. Furthermore, EXCEL and some FORTRAN codes which were written during the project, are used for converting the physical, chemical and thermodynamic data for calculations. The validation of the chemical kinetics with real process is done by comparison between an experimental data. Gelling and blowing reaction rates are adjusted with the calibration of the Arrhenius parameters. Thus a similar behavior obtained with real reactions.

KATILAŞMA SÜRECİ OLAN POLİÜRETAN KÖPÜK AKIŞNA GÜRE YENİ BİR BUZDOLABI KABİNİ TASARIMI

ÖZET

Uluslarası piyasada rekabet hızla büyümekte firmalar enerji verimliliği konusunda yarışmakta ve bu konu üzerine büyük yatırımlar yaparak AR-GE çalışmalarını sürdürmektedirler. Poliüretan kullanım alanı bakımından çeşitlilik göstermesinden ve son ürününün özelliklerini değiştirmek çok kolay olduğundan, uluslarası piyasada gün geçtikçe daha fazla önem kazanmaktadır. Bu yarış buzdolabı üreticileri arasında da güçlenmektedir. Enerji verimliliği yüksek bir buzdolabının ısıl yalıtım kabiliyetlerinin de yüksek olması gerekmektedir. Buzdolaplarında ısıl yalıtımı sağlamak için kabin duvarları içerisinde katı poliüretan köpük kullanılmaktadır. İyi bir yalıtıma sahip buzdolabı kabininde poliüretan köpük; kabinin her yerine homojen şekilde dağılmalı, poliüretan köpüğün yalıtım ve mekanik dayanım özellikleri istenen şartları sağlamalı, kabin dolum süresi mümkün olduğu kadar kısa olmalı ve bu kısıtlar sağlanırken köpük üretiminde kullanılan kimyasallara yapılan harcamalar en aza indirilmelidir. Poliüretan üretimi görece düşük maliyetli olmasa da, uygulanabilirlilik üstünlükleriyle aynı alanda kullanılan malzemelere tercih edilir hale gelmişlerdir. Örneğin; poliüretanların çeşitli kalıplara basılmasında dolum benzer işlemlere göre daha düşük basınçlar olmasından dolayı kalıp malzemeleri çelik yerine daha ucuz olan alüminyum, polyester hatta plastik kökenli malzemelerden üretilmektedir. Bu üretimi hızlandırdığı gibi , süreç geliştirme çalışmalarına esneklik kazandırmaktadır. Bütün bunların sağlanabilmesi için buzdolabı kabinlerine poliüretan basım işleminde kabin içerisinde hapsolan havanın çıkabilmesi için gerekli olan hava çıkış deliklerinin yerleri, sayıları ve boyutları, tepkimelerin gelişimi, poliüretan köpüğün ilerlediği kanalların yapısı, kalıp içerisine püskürtülen malzemenin sıcaklığı ve kalıp sıcaklığı işlemin performansını belirleyen değişkenlerdir. Bu değişkenlerin en iyileştirilmesi fiziksel sürecin iyice anlaşılmasına bağlıdır. Ancak bu sayede buzdolabına poliüretan basım işlemi üzerinde en üst derecede kontrol sağlanabilir ve gelecekte üretilmesi planlanan buzdolaplarında yukarıda bahsi geçen değişkenler işlem öncesinde yaklaşık olarak belirlenmesiyle; poliüretan basım süresinden ve süreçte kullanılan malzeme harcamalarından kazanım sağlanır ve işlem verimli bir şekilde uygulanabilir.

Katı poliüretan köpük eldesinde izosiyanat ve poliol karıştırılması ile başlayan tepkimelerle, karışım hacmi başlangıçtaki hacminin yaklaşık 30 katına kadar genişlemektedir. Genelde kimyasal tepkimeler tek adımda gerçekleşiyor gibi görünse de aslında bir çok ara tepkime sonrasında son ürünler elde edilmektedir. Uygulamada sadece izosiyanat ve poliolün birtakım katkılarla birlikte karıştırılmasından elde edilen poliüretan köpük birden fazla ara tepkimenin ürünlerinin birleşimidir. Birden fazla ve aynı anda gerçekleşen bu tepkimelerin çoğu ısı veren tepkimelerdir. Tepkimelerden açığa çıkan ısı ile tepkimelerin devamlılığı ve kürlenme sağlanmaktadır. Tepkimelerin hangi oranda ve hızda gerçekleşeceği ise katalizörler ile kontrol edilmektedir.

Poliüretan tepkime modeli 11 adet tür ve 5 adet tepkime ile oluşturulmuştur. Bu türlerden dokuzu tepkimelerle değişmekte kalan ikisi ise tepkime modeline girdikleri gibi çıkmaktadır. Tepkimelere girdikleri gibi çıkan hava ve fiziksel kabartıcıdaki değişimler kimyasal değil fiziksel değişimlerdir. Tepkime kinetiği modeline eklenmelerinin sebebi, hesaplama hacminde üzerlerine çektikleri ısıyı tepkime kinetiği modelinde gözlemleyebilmektir. Bir hesaplama hücresindeki toplam entalpi; hücre içerisinde bulunan türlerin entalpilerinin kendi kütle oranlarıyla çarpılıp, daha sonra hepsinin toplanmasıyla bulunmaktadır.

Poliüretan akışında çalkantı beklememekle birlikte genişleyerek ittiği hava akışında oluşabilecek çalkantı için Unsteady Reynolds Averaged Navier-Stokes (URANS) ile eklentili $k-\varepsilon$ modeli kullanılmaktadır. Buzdolabı kabininin katı poliüretan köpükle doldurulma sürecinde hava tarafı çalkantılı akış özelliğindedir.

İki kapılı buzdolabı için hesaplama ağı ANSYS Meshing yazılımında Cutcell yöntemi kullanılarak atılmıştır. Bu yöntem sayesinde HAD hesaplamaları için karmaşık geometrilerin uzaysal ayrıklaştırılması daha kolay hale gelmiştir. HAD çözümlerinde FLUENT 6.3 yazılımı kullanılmıştır. Tepkime kinetiği modeli HAD yazılımına dışarıdan çağrılarak tepkimeli akış modellenmiştir. Bu işlem HAD yazılımı içerisine Kullanıcı Tanımlı Fonksiyonlar (UDF) sağlanmıştır. Kabin içerisine türler belirli kütle oranlarında karıştırılarak 8.66 saniye boyunca 1.5 kg/s debiyle basılmaktadır. Basılan türlerin sıcaklığı 21°C'dir. Gerçek süreçte kabin türler basılmadan önce 40°C'ye kadar ısıtılmaktadır. Sıcaklığın tepkimelere olan hızlandırıcı etkisine geçmiş bölümlerde değinilmiştir. Buna göre malzemenin kabin ile temas eden bölgelerinde tepkimelerin daha hızlı gerçekleşmesi beklenmektedir. Kabin içerisine basılan karışım içerisindeki tür kütle derişimleri; Ysu = 0.0095, Yizosiyanat = 0.57, Ypoliol = 0.3705, YFK = 0.05'dir.

Bu bilgilerin ışığında ARÇELİK A.Ş ile SAN-TEZ 01213.STZ-2012-1 adı altında bir proje başlatılmış ve iki kapılı bir buzdolabı benzetimlerde kullanılmak üzere seçilmiştir. Yukarıda söz edilen en uygun koşulların saptanması için bu buzdolabı kabini içerisine poliüretan basım işleminin hesaplamalı akışkanlar dinamiği (HAD) benzetimleri yapılmıştır. Söz konusu fiziksel süreç zamana bağlı, üç boyutlu, tepkimeli, çalkantılı ve çok fazlı akış niteliğindedir. Kabin içerisindeki akış kimyasal tepkimelerden etkilenmektedir. HAD benzetimlerine ek olarak poliüretan köpük oluşum tepkimelerinin kinetikleri akış olmadan sadece yerel olarak incelenmiş ve en uygun işletim koşullarının saptanması amaçlanmıştır. Kabin geometrisi için örülen çözüm ağları sonlu hacimler yöntemi ile ANSYS MESHING ve ICEM CFD yazılımları ile oluşturulmuştur. Geometri üzerindeki çeşitli iyileştirmeler SOLIDWORKS ve CATIA yazılımları kullanılarak yapılmıştır. Bunun yanında tepkime kinetiklerinin modellenmesi için FORTRAN programlama dilinde yazılmış ve İTÜ Akışkanlar Grubu içerisinde geliştirilmiş, kimyasal tepkimelerin kinetiklerini çözen bir yazılım kullanılmıştır. HAD benzetimleri FLUENT yazılımında gerçekleştirilmiştir. Tepkime kinetiği çözüm içerisine kullanıcı tanımlı fonksiyonlar (UDF) aracılığı ile dışarıdan ilintilenerek; FLUENT ve tepkime kinetiği yazılımı eş zamanlı çalıştırılmıştır. Hesaplamaların sonuçları TECPLOT ve MATLAB yazılımları kullanılarak görselleştirilmiştir. Buna ek olarak tepkimeye giren türlerin fiziksel, kimyasal ve termodinamik özelliklerinin hesaplamalarda kullanılacak biçime getirilmesinde EXCEL yazılımı ve proje süresince yazılmış birtakım FORTRAN

kodları kullanılmıştır. Yapılan hesaplamalar sonucunda buzdolabı kabinine poliüretan basım sürecinin daha verimli hale getirilmesi için önerilerde bulunulmuştur. Gelecek çalışma planı, önerilen iyileştirmeler doğrultusunda yeni bir kabin geometrisi hazırlanarak, HAD benzetimlerinin yapılmasıdır. Yeni tasarımla yapılan benzetimlerle, bu çalışmadaki benzetimler karşılaştırılıp iyileşmeler gözlemlenecek ve sonuçlar doğrultusunda eski ve yeni tasarıma poliüretan basımı yapılarak HAD sonuçları ile önerilen düzeltmelerin gerçek buzdolabı geometrisinde sağladığı iyileştirmeler gözlemlenilecektir. Sonuç olarak süreç kişiden kişiye aktarılan tecrübelere ek olarak bu çalışmada elde edilen bilgi birikimi ile gerçekleştirilerek, uluslararası pazarda rekabetçi teknolojik ürünlerin geliştirilmesi yolunun açılması amaçlanmaktadır.

1. INTRODUCTION

The foundations of polyurethane industry was introduced in the late 1930s by Otto Bayer who discovered the chemistry of the poly-addition reaction between diisocyanate and diols to form polyurethane. The first applications of the polyurethane polymers was millable, coating, adhesive which were developed between 1945 and 1947. Then the flexible foams were introduced in 1953 and rigid foams were introduced in 1957. Since then the application of polyurethane has been spread. Flexible foams are used in comfortable automotive and domestic seating. The low thermal conductivity of rigid polyurethanes is exploited in insulation industry which is used in the refrigerator and industrial buildings [2].

Basically, the production process of the polyurethane is an exothermic reaction of molecules containing two or more isocyanate groups with polyol molecules which contains two or more hydroxyl groups. The production process of the polyurethane contains a few basic isocyanate and a wide range of the polyols with different molecular weight to produce a wide variety of polyurethane materials.

The commercial application of the polyurethane is very wide. Fig1.1 shows the most common applications of the polyurethane which are divided into seven major parts. Rigid foams, solid elastomer, flexible foam, flexible molded foam, RIM, carpet backing and two component formulations [1]. Types of polyurethane foams can be divided into flexible polyurethane foams and low-density rigid polyurethane foams. The main difference between these two types is that flexible polyurethane foams allow air to move freely through the material when flexed that will lead to excellent sound absorption and heat resistance because of low thermal conductivity. Moreover, the flexible foam can be classified as low-density flexible polyurethane foam and high-density flexible polyurethane foam. Low-density flexible polyurethane foam have density range 10 to 80 kg/m^3 with open cell macro. Air has no hinder to pass through the adjacent cell in the foam structure. The low-density foams are those with closed

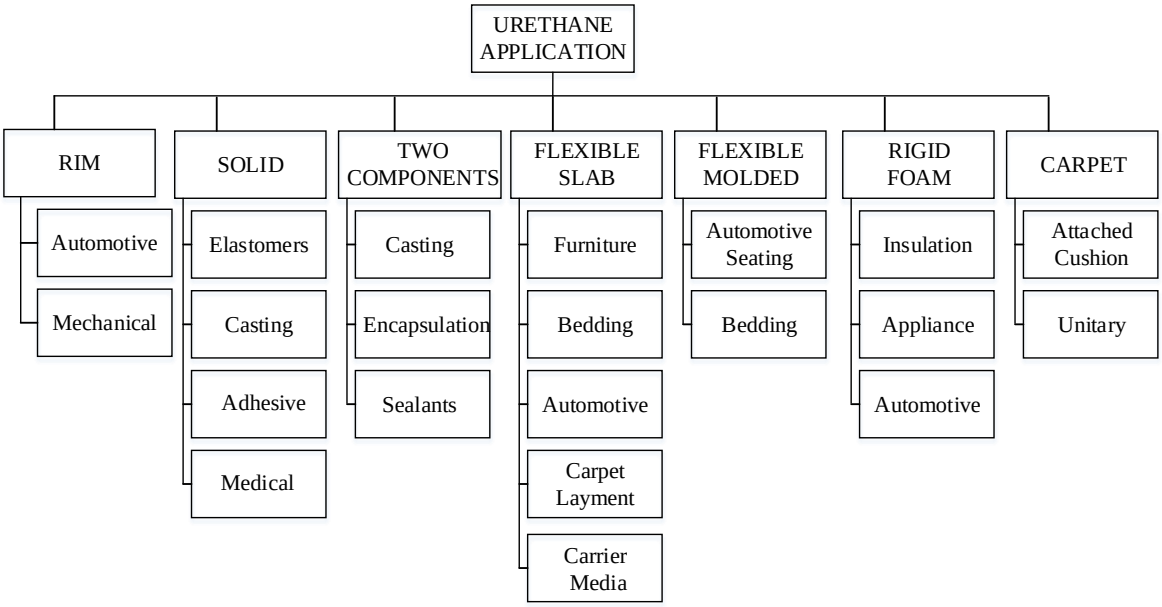

Figure 1.1: Universal application of polyurethane [1].

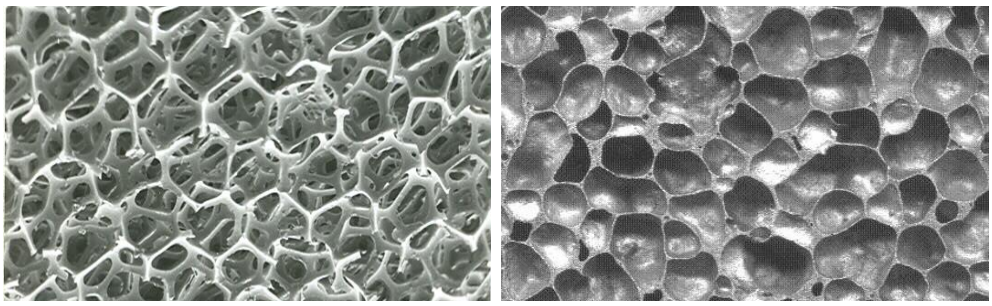

Figure 1.2: Open and closed polyurethane foam cell structure.

cell structure with density range 28 to 50 kg/m^3 [2]. The adjacent cells are separated from each other by tin polymer walls that are hinder to air and gas flow through the foam cell structure after. Therefore, gas will be trapped into the foam structure to make it a great thermal insulator which is used in the refrigerator industry Fig1.2.

When the isocyanate and polyol blend are mixed together, there is almost 30-time increase in volume during the reaction. Choosing correct surfactant has a significant impact on cell formation. So that incorrect surfactant choosing leads to higher degree of open cells. The rigid foam polymer structure will be self-supporting which means that there is enough network formation and the foam expansion is supported by the internal cell gas pressure and external atmospheric pressure. Once the foam has enough strength to persist against pressure difference, the expansion will stop [2].

The foaming process can be defined in several time stages which begins with the start of mixing known as the mixing time as the first zero time stage then it goes to cream time, gel time, tack-free time and end of rise time [2]. At the cream time, the mix starts to foam. Gel time is the time when the expanded foam begins to polymerize or gel. It is recognized by touching the expanded foam (with gloves or tools) and noticing a thin polymer strand or string. At the tack-free-time the surface of foam stops being tacky and the end-of-rise time is the time for maximum foam height. Different time stages of the foaming process is shown as Fig 1.3 and Fig 1.4.

According to Fig1.3 the cream time starts as soon as mixing starts where time is close to zero. It take almost 55-60 s to foam to pass Gel time, track-free time and reach to End-of-rise time stage that is maximum height that foam can reach at almost 180-190 °C, which is the maximum temperature for foam center. At this point the foam will stop rising and become more stable. The average foam expanding velocity from zero to maximum height (30 cm) which happens at first 60 s could be find as 0.5 cm/s.

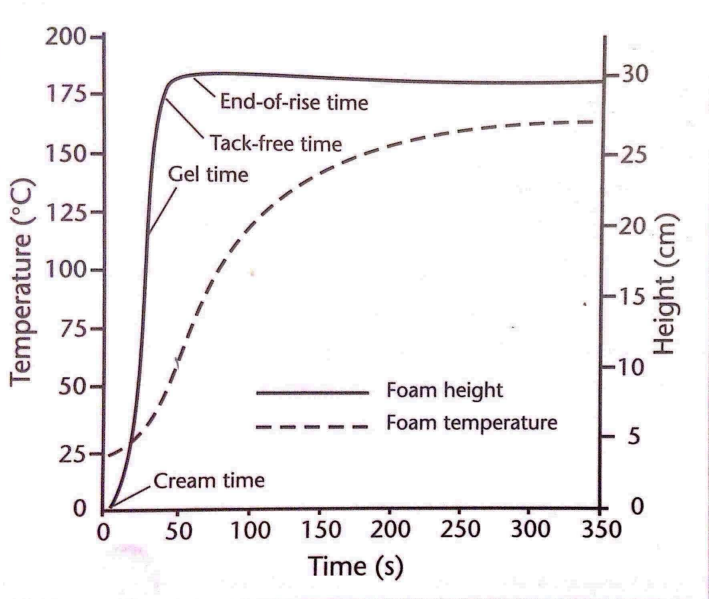

Figure 1.3: Evolution of temperature and foam height versus time [2].

The cream and gel times are the critical measures for different applications. The cream time should be longer than then injection time to let the foam expands and fills the cabinet. For appliance systems, the gel time normally occurs when the foam has reached about the 85 percent of its final free expansion time. The difference between

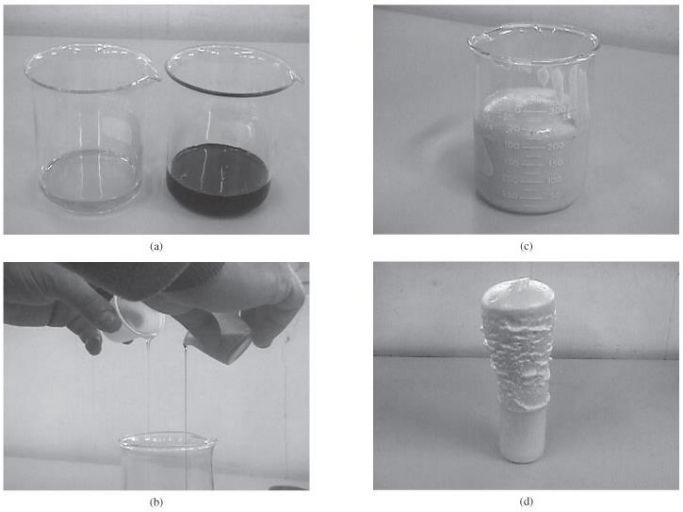

Figure 1.4: Laboratory foam rising test.

cream and gel time also determines the speed at which the foam will develop during its expansion process in the cavity.

The free-rise density is also very important parameter because it determines the expansion capability of the foam and hence the final overall density in the cabinet or door. The free-rise density of foam used to fill appliance is generally between 21 and 25 kg/m^3, depend on the blowing agent used, with the final overall core foam density typically between 28 and 34 kg/m^3.

One of the most important properties of rigid polyurethane foam is low thermal conductivity which is defined by heat transfer rate from specific thickness.The thermal conductivity is measured on a piece of foam. foam samples used for these measurements have the foam skin removed and only provide the performance of the specific test sample. Since the foam quality in the cabinet will vary, the thermal conductivity will also vary and will be dependent on the position it is taken from within the cabinet. The thermal conductivity remains a good indication of the total insulation properties of the foam in a cabinet and is quick and easy to measure. The total thermal conductivity of the rigid foam has 4 main parts which are radiative, solid, gas and convection. The convection term of the thermal conductivity could be ignored due to small cell diameter. Therefore, the thermal conductivity is changing from foam to foam by considering radiative , gas and solid parts Fig1.5.

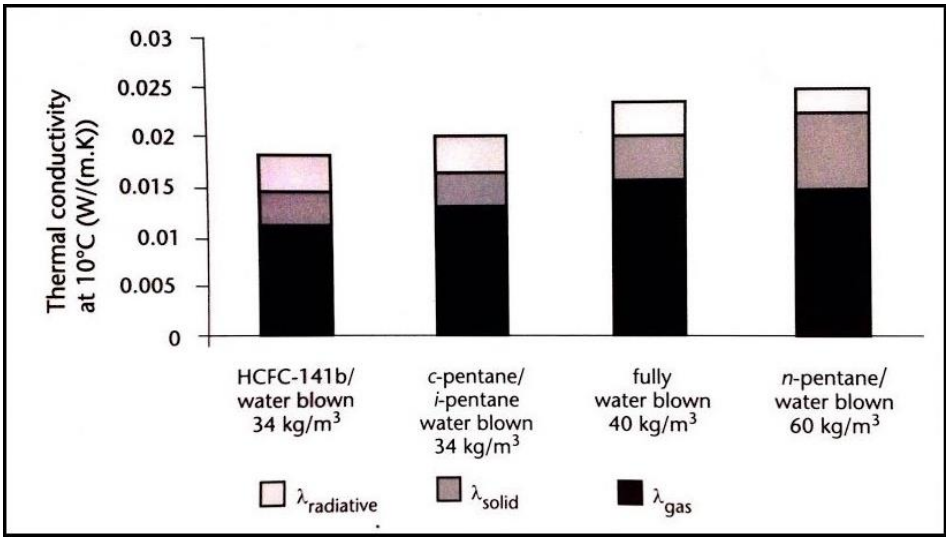

Figure 1.5: Thermal conductivity split into three parts [2].

Radiative thermal conductivity defined as $\lambda_{radiative}$ will increase by increasing density due to much more material presence. $\lambda_{radiative}$ depends on temperature directly which will increase significantly with increasing temperature. λ_{gas} is the conductive part of heat transfer through the gas phase. All the physical blowing agents as well as carbon dioxide have much lower λ_{gas} than air. Generally λ_{gas} decreases with increasing molecular weight of the gas but increases with increasing temperature.

Foam aging is another aspect that should be considered. For fresh foam there were physical blowing agent and carbon dioxide with some amount of air at the cell gas composition. The pressure differences will cause air to inter to the foam gradually by the time. Moreover, the physical blowing agent and carbon dioxide will move out of the foam by foam ageing due to difference in partial pressure as shown in Fig1.6 and Fig1.7.

The enterence of air causes an slight increase of thermal conductivity where the air has a much higher λ_{gas} than physical blowing agents. The equality of internal partial pressure to external atmospheric partial pressure will stop air permeation. the thermal conductivity will also reach a plateau level. The differences between plateau level and initial level is changing from 0.004 to 0.007 W/(m.k), depending on physical blowing agent type that is used.

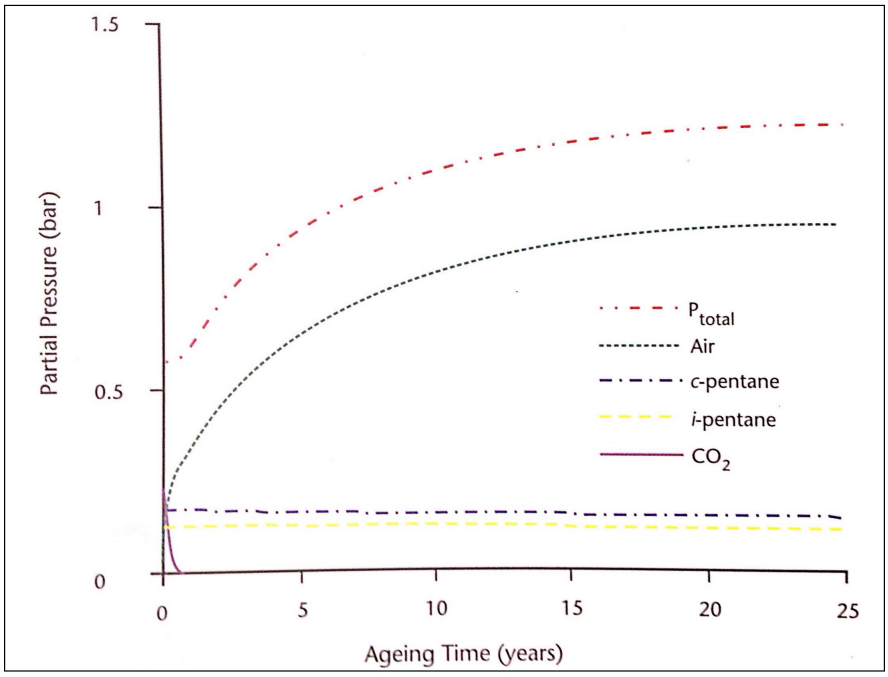

Figure 1.6: Cell gas partial pressure versus ageing time [2].

1.1 Purpose of Thesis

Several complex phenomena such as chemical reactions, heat generation and blowing agent evaporation should be considered in the study of polyurethane foam formation process [6]. Thus, there are several expensive experimental runs and prototypes that should be done to understand the polyurethane injection with solidification process in the refrigerator complex geometry. The purpose of this study is to find a method to analyze the model of polyurethane injection process in a refrigerator cavity by considering some known parameters and operating conditions such as initial temperature, the amount of material that should be injected, posture of the cabinet, the position, size of the inlet hole, the structure of channel in which the flow pass with in and the position, size and number of outlet holes before highly expensive experimental tests to decrease time to market cycle and of course reduce costs by using fewer prototypes. Moreover,this study leads to better understanding about the nature of multiphase, turbulent and 3D reactive flows.

1.2 Literature Review

Design and Modeling of manufacturing processes based on filling molds with polyurethane foams still require the use of highly empirical approaches, which is

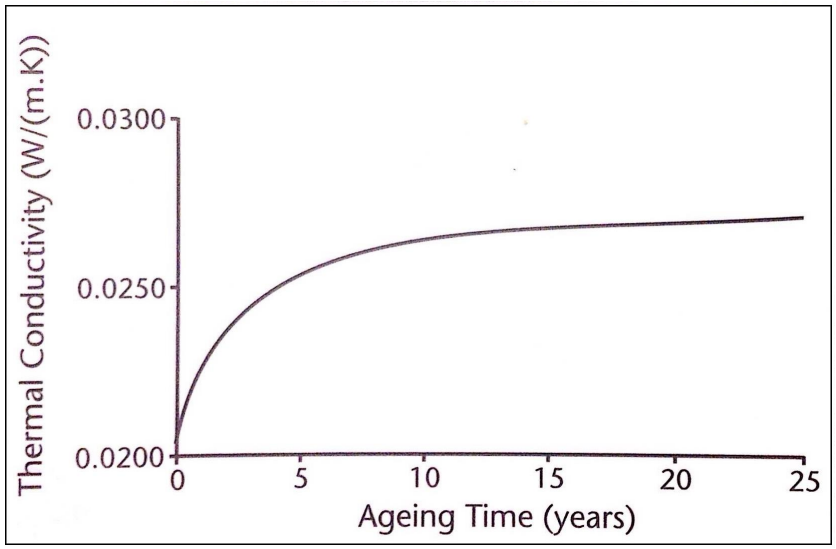

Figure 1.7: Thermal conductivity versus ageing time [2].

expensive and time consuming so numerical approach is needed as a framework for understanding of polyurethane formation to reduce the cost of mold design [6]. There are a lot of studies that are considering the mold filling process that include the concept of the reaction kinetics in less complex geometries.

One of these studies is [7], which modeled the dynamic of a physical blowing agent and water. Water is the chemical blowing agent for polyurethane. The rates of chemical and physical blowing agents control the dynamic of the foams. The temperature and density change were observed by experimental run during the foaming. It is observed that, the temperature and density change as a function of time. Heat generation and carbon dioxide production will be happened as the result of this exothermic reaction. Heat generation is controlled by physical blowing agent and the amount of carbon dioxide is controlled by percentage of the water.

The other study is [6], which used numerical approach for simulation of mold filling. The VOF (volume of fluid) model has been used to capture foam front by using OpenFOAM. Moreover, foam is considered as a compressible and two phase (ideal foam and air) flow. Phases is separated by a sharp interface using VOF model. The viscosity increased and thermal conductivity reduced during the foaming. It is an exothermic reaction which increases the temperature of the foam. CO_2 production causes expansion od the foam and gelling and blowing are two primary reactions and heat is degenerated by evaporation of physical blowing agent. An adiabatic mold cavity

is considered to verify the numerical implementation of self expansion foam flow. Three different analysis are done to investigate the effects of different combination of blowing agents on reaction rate. The results are showing that presence of water as the chemical blowing agent accelerates the reaction by rising the temperature, while physical blowing agent postpones the reaction (endothermic reaction). When isocyanate reaches to gel point, foam viscosity increases rapidly. The effect of gravity on foam is observed. Gravity causes the foam front become more flat. A Korean group developed a numerical method for unsteady three dimensional (3D) simulation of rigid polyurethane (PU) foaming flow in a refrigerator cabinet in [8] which is assumed to have time-variant density and viscosity, without considering the chemical reaction, using finite volume method for numerical methods. Air in a refrigerator cabinet is neglected in the numerical method, and the free surface is traced with the volume of fluid (VOF) method.Viscosity and density of foam are assumed to be uniform in space and time-dependent, which are obtained with experimental methods. The results of numerical simulation compared with experimental results. Ignoring the effects of chemical reaction during the foam flow is the weakness of this study. The chemical reactions has been considered in [9] but not appropriately and the air flow in front of the foam flow is not studied very well . Finite element method (FEM) has been used as the numerical method in [10]. The validity of the model is investigated by applying it to the Hele-Shaw formulation, which assumes that the cavity is very thin compared to its width. the Volume of Fluid (VOF) method is applied to predict the flow front advance. Prediction of flow patterns of the three molds with different gap thickness has been done and compared with experimental results. Flow front progressed more slowly where the gap was narrower. To apply finite volume method, the volume should be discretized into millions of small grids which is called meshing process. In this project, Cutcell mesh methods has been used which is very fast and gives very precise results. The curtecisan mesh method has been studied in [11]. The cell merging process not only keeps the shape resolution as good as before merging, but also makes both the location of cut face center and the construction of interpolation stencil easy and systematic, hence enables the straightforward extension to three dimensional space in the future. Various test examples, including a moving-body problem, were computed and validated against previous simulations or experiments to prove the accuracy and

effectiveness of the present method. The observed order of accuracy in the spatial discretization is superlinear. But, another study introduced a software with no need for grid generation which is called NOGRID, where can help to understand the flow inside the cavity. It can show the entrapment of air, the density distribution of the isolation material and the pressure of the PU foam acting on the cavity. NOGRID unites abilities to handle free surface flow and moving parts in the domain and allows the simulation of any conceivable refrigerator geometry and operation modes such as PU injection by one or more inlets, moving parts and inlets,free definable PU properties by equations or curves and large refrigerator geometries with small gaps or cutouts [12]. the results are not as good as finite volume method or finite element methods, but it could be used as a fast alternative to get quick results.

2. POLYURETHANE CHEMISTRY

2.1 Reaction Components

Polyurethanes formation is the reaction of polymerization of isocyanate with active hydroxyl compounds [13]. During the polyurethane foam formation several exothermic reactions happen simultaneously which are good energy source to drive mold filling and foaming. Catalysts are used to balance the rates and speed of various reactions. Further reactions are shown as Fig 2.1.

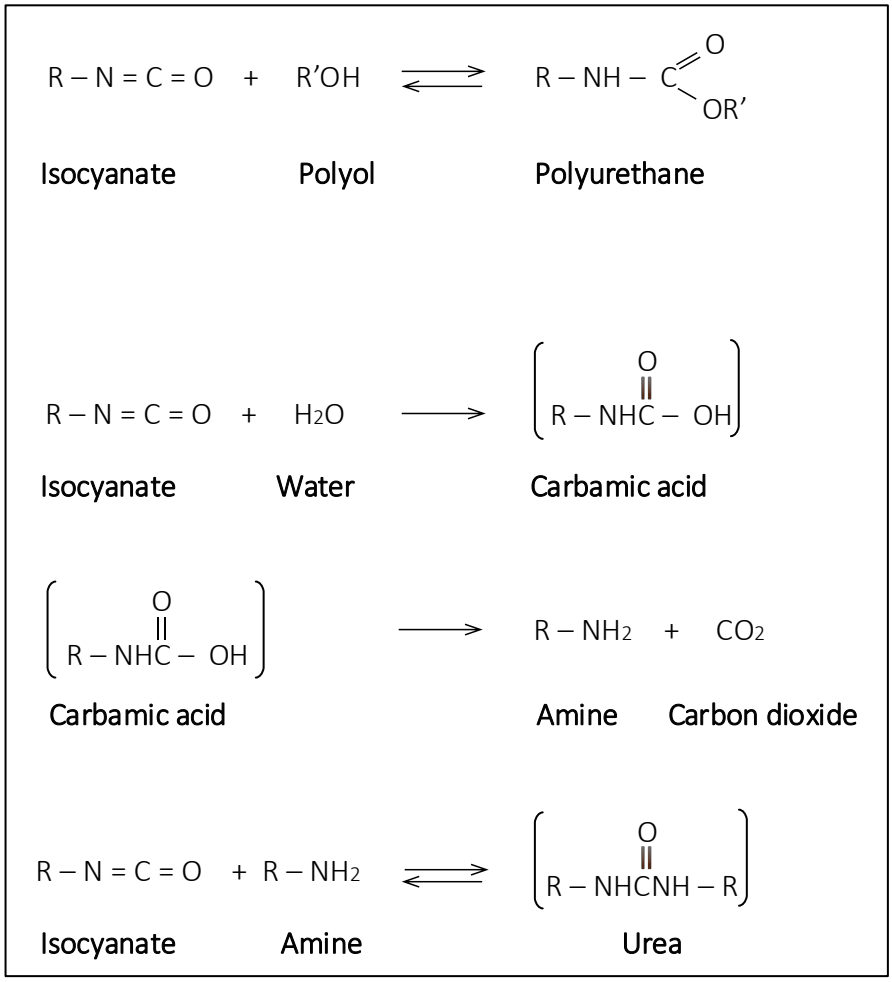

Figure 2.1: Further reaction for the formation of rigid polyurethane foams [2].

2.1.1 Isocyanate

The most critical characteristic of the isocyanate is to be highly reactive that is very important for chemistry of polyurethane [1]. The reactivity level of isocyanate changes by the electronic structure of isocyanate. For example, aromatic isocyanate such as MDI and TDI are more reactive than aliphatic isocyanate like HDI and IPDI. MDI as an aromatic isocyanate is used to obtain the rigid polyurethane foam [2]. Compression resistance, law thermal conductivity can be said as the MDI properties.

2.1.2 Polyol

Polyol is another important species in the polyurethane chemistry. In the first global reaction, isocyanate reacts with polyol to form polyurethane which is called gelling reaction [13] as shown as the first reaction of Fig 2.1.

2.1.3 Water

The reaction of isocyanate and water is highly exothermic which produces carbamic acid firstly, the carbamic acid is unstable and spontaneously decomposes into amine and carbon dioxide which is called blowing reaction and water is known as the blowing agent where a change of the amount of water has a very big impact on the polyurethane formation because it changes the level of the blow. The reaction of amine to another isocyanate group will rapidly produce urea as shown as the second reaction of Fig2.1. The reaction rate depend on temperature, water concentration and catalyst [14]. The exothermic reaction of isocyanate and and water is slow without catalyst because water is not very soluble in isocyanates such as MDI and TDI. If we consider the amount of water in the reactions carried out in the refrigerator, the mass ratio of water to polyol in the pre-mixed water polyol mixture is about 2.5% that is reported by the manufacturer. The density of the foam decrease as water mass fraction increases. Moreover, increasing the mass fraction of water will cause an increase in the blowing reaction and the urea production will increase consequently.

2.1.4 Urea

Hard structures will be formed in the Foam which are called the urea balls. The urea structures will be gathered together in the certain points of the mix which causes to phase separation. Experimental studies show that during the foaming process, the hard and soft structures are grouping themselves separately. This structure of the urea is shown as Fig 2.3. The distance between urea balls are almost 3000 Angstrom (1Å= 10^{-10}m).

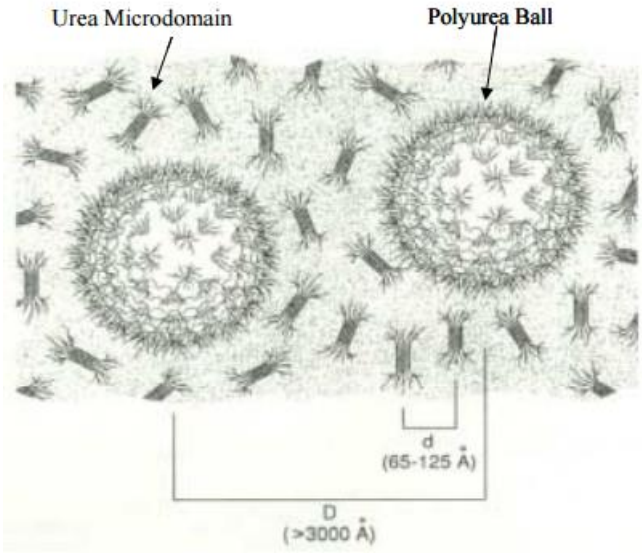

Figure 2.2: The phase separation behavior in polyurethane foams [3].

2.1.5 Physical Blowing Agents

CFC's and HCFC's are ideal blowing agents but they are forbidden in many countries due to the tremendous environmental concerns associated with them. In this project, C70 will be used as the physical blowing agent where its boiling point is 50 °C [15]. The physical blowing agent (C70) will not participates in the reaction but it will exit the reaction with phase change. In fact, the liquid physical blowing agent changes to gas phase at the early stages of the reaction due to low boiling point and it will speed up the blowing process. Moreover, due to low thermal conductivity they will be trapped into the foam shells and provide great thermal insulation. Density and hardness drop was observed when the amount of the physical blowing agent was increased. Moreover, the

generated heat as a result of exothermic reactions is a source for the evaporation of the physical blowing agent. Hence the maximum temperature of the reaction is decreased because of the phase change for physical blowing agent and the thermal distortion for both foam and refrigerator cabinet is low consequently.

2.1.6 Modeling of Reaction Kinetics

The polyurethane reaction model is created by 11 species and 5 reactions. Nine of these species has chemical bound change with the reaction but for two other spices phase change is observed without participating in the reaction. The change for physical blowing agent and air is not chemical but physical. The air and physical blowing agent should be considered during the modeling of reaction kinetics while they only have phase change. The reason is that they absorb the heat that is generated as the result of exothermic reactions. The total enthalpy for a single cell can be calculated as the summation of the enthalpy of every species multiplied by the mass fraction of that species in the cell. According to Fig2.3, a new step has been added to the polyurethane reactions while the reactants and products of this step (air and PBA) are same chemically but their temperatures are different.

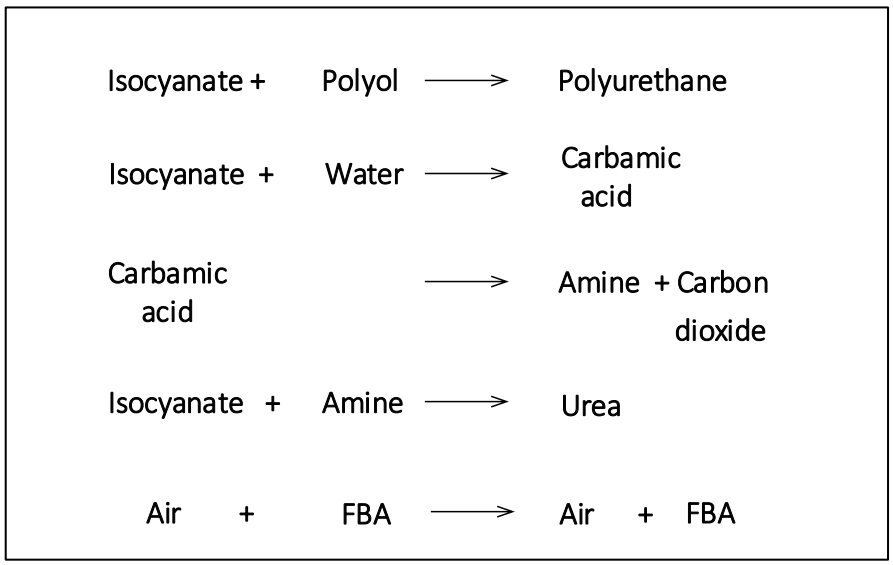

Figure 2.3: Reaction kinetics model steps.

Generally, a chemical reaction can be expressed as follow:

$$\sum_{k=1}^{K} \nu'_{ki}\, \chi_k \longrightarrow \sum_{k=1}^{K} \nu''_{ki}\, \chi_k \qquad i = 1,..,l \tag{2.1}$$

where χ_k is species, ν'_{ki} and ν''_{ki} are stoichiometric coefficients of the reactants and products respectively, K total number of the species and i represents the total number of the primary reaction. The total production rate of the species $\dot{w}_k$:

$$\dot{w}_k = \sum_{i=1}^{l} \nu_{ki}\, S_i \qquad k = 1,...,K \tag{2.2}$$

$$\nu_{ki} = \nu''_{ki} - \nu'_{ki} \tag{2.3}$$

s_i as the source term of the species for each species can be defined as:

$$s_i = k_{fi} \prod_{k=1}^{K} [X_k]^{\nu'_{ki}} - k_{ri} \prod_{k=1}^{K} [X_k]^{\nu''_{ki}} \tag{2.4}$$

Where X_k is the molar concentration of the k'th species, k_{fi} and k_{ri} are the forward and backward reaction rates.

The forward reaction rate constant can be find from the Arrhenius equation:

$$k_{fi} = A_i T^{\beta_i} exp(\frac{-E_i}{RT}) \tag{2.5}$$

Where k is the reaction rate constant, E_a is the activation energy, A_k is the pre-exponential factor, β is temperature base, R is the universal gas constant and T represents temperature.

The backward reaction rate dependent on forward reaction rate can be defined as:

$$k_{ri} = \frac{k_{fi}}{K_{ci}} \tag{2.6}$$

Where K_{ci} represents the equilibrium constant. To calculate the equilibrium constant, we can benefit from the thermodynamic properties of the pressure unit as follow:

$$K_{ci} = K_{pi}\left(\frac{P_{atm}}{RT}\right)^{\sum_{k=1}^{K} \nu_{ki}} \tag{2.7}$$

and K_{pi} as a function of pressure:

$$K_{pi} = exp\left(\frac{\Delta S_i^0}{R} - \frac{\Delta H_i^0}{RT}\right) \tag{2.8}$$

Where, Δ represents the transfer of reactants to products for i'th reaction. Therefore, ΔS_i^0 is the transfered entropy from reactants to products and ΔH_i^0 represents the transfered enthalpy. To calculate them:

$$\frac{\Delta S_i^0}{R} = \sum_{k=1}^{K} \nu_{ki} \frac{S_k^0}{R} \tag{2.9}$$

$$\frac{\Delta H_i^0}{RT} = \sum_{k=1}^{K} \nu_{ki} \frac{H_k^0}{RT} \tag{2.10}$$

The above mentioned formulas are the general representations of the entropy and enthalpy. In this project, these variables are calculated depending on the temperature as follows [15]:

$$\frac{C_{pk}^0}{R} = a_{1k} + a_{2k}T_k + a_{3k}T_k^2 + a_{4k}T_k^3 + a_{5k}T_k^4 \tag{2.11}$$

$$\frac{H_k^0}{RT_k} = a_{1k} + \frac{a_{2k}}{2}T_k + \frac{a_{3k}}{3}T_k^2 + \frac{a_{4k}}{4}T_k^3 + \frac{a_{5k}}{5}T_k^4 + \frac{a_{6k}}{T_k} \tag{2.12}$$

$$\frac{S_k^0}{R} = a_{1k}lnT_k + a_{2k}T_k + \frac{a_{3k}}{2}T_k^2 + \frac{a_{4k}}{3}T_k^3 + \frac{a_{5k}}{4}T_k^4 + a_{7k} \tag{2.13}$$

Where, C_{pk}^0 refers to specific heat constant at the constant pressure for k'th species. Specific heat, enthalpy of formation and entropy are given for spices at the above mentioned expressions. To make practical use of Eqn. 3.12, we have define a standard reference state for enthalpy calculation. We employ T_{ref} = 25°C, as the standard-state temperature and $P_{ref} = P^0 =$ 1atm (101,325 Pa), as the standart-state pressure [16].

2.2 Tuning Model Parameters

The modeling of reaction kinetics has been done according to the Fig2.1 using FORTRAN programming language. The main variables that determine the reaction kinetics are Arrhenius variable (A_i, β_i, E_i) and given (3.11), (3.12) and (3.13) polynomials. The physical process of the reaction is affected directly by density and viscosity. Similar to the specific heat, enthalpy and entropy, Species density and viscosity are calculated depending on the temperature by using high order polynomials. The polyurethane foam density which has given by the manufacturer is 35 kg/m^3. Thus the initial condition for the polyurethane injection process in the two door refrigerator are as below:

$$T_{cabinet} = 313.15[K]$$

$$t = 350[s]$$

$$Y_{water} = 0.0095$$

$$Y_{isocyanate} = 0.57$$

$$Y_{polyol} = 0.3705$$

$$Y_{PBA} = 0.05$$

Where, T_g is the initial temperature of the reaction and Y refers as mass fraction. For example, Y_{PBA} is mass fraction of physical blowing agent. Calculations are shown with a total time of t and the sum of species mass fraction is 1. During the modeling of reaction kinetics , given species mass fraction is turned out in its molar fraction and it changes to mass fraction again at the end of the reaction. The relations between mass fraction and molar fraction are as follows:

$$Y_i = \frac{M_i n_i}{\sum_{j=1}^{S} M_j n_j} = \frac{M_i X_i}{\sum_{j=1}^{S} M_j X_j} \tag{2.14}$$

$$X_i = \frac{Y_i}{M_i}\overline{M} = \frac{M_i/Y_i}{\sum_{j=1}^{S} M_i/Y_i} \tag{2.15}$$

Where S denotes the number of different compounds, Y_i is mass fraction, M_i is molar mass, the mean molar mass of a mixture $\overline{M}$ (in g/mol, e. g.) denotes an average molar mass, using the mole fractions as weight ($\overline{M} = \sum M_i X_i$) [17]. Figure 2.4 shows the change in density as a function of time obtained by reaction kinetics model.

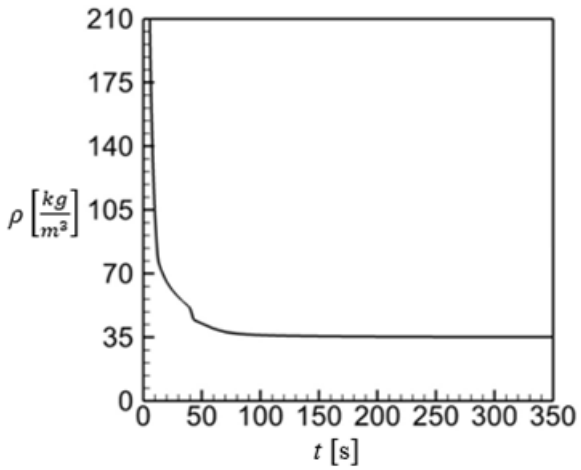

Figure 2.4: Density change as a function of time.

The density of species has been found depending on the temperature for every instance for every calculation space. In the model of reaction kinetics, species varies depending on time and space, new enthalpies of species are calculated by considering local positions and generated heat of ongoing reactions and the thermodynamic data is used to detect locally changing temperature. Fig 2.4 shows that for density 1837.78 kg/m^3 at t = 0 s, the curve is laid outside the graph and that is because it was intended to have a more clear analysis of density behavior at about 35 kg/m^3. Fig 2.4 shows that the density decreases rapidly at first 55-60 s, then it remains constant until the end of the process. Hence it is equal to the value in the rigid polyurethane catalog given by the manufacturer.

Dynamic viscosity, or simply the viscosity of the fluids is the fluid property that relates shearing stress and fluid motion [18].

$$\tau \propto \frac{du}{dy} \tag{2.16}$$

$$\tau = \mu \frac{du}{dy} \tag{2.17}$$

Plot of τ versus $\frac{du}{dy}$ should be linear with the slope equal to the viscosity. Where τ is shear stress, u is velocity and μ is viscosity. The shear stress during the polyurethane rigid foam expansion process is the result of forces which are caused by trapped gases into the foam cells plus density.The dynamic viscosity change versus time which shows that the viscosity has very fast growth at first 50 s and it has almost maximum value at 55-60 s. Therefore, the moment at which the expansion of the foam has stopped can be said as the point for maximum viscosity.

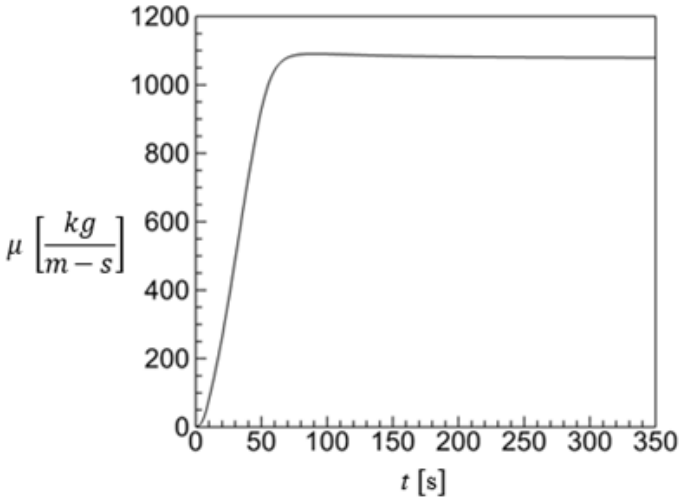

Figure 2.5: Dynamic viscosity change as a function of time.

3. COMPUTATIONAL FLUID DYNAMICS (CFD)

Computational fluid dynamics, CFD, is a branch of fluid mechanics that uses numerical methods to solve partial differential equation (PDEs) problems that involve fluid flows. The objective of CFD is to analyze PDEs by solving algebraic equations using numerical methods Fig 3.1.

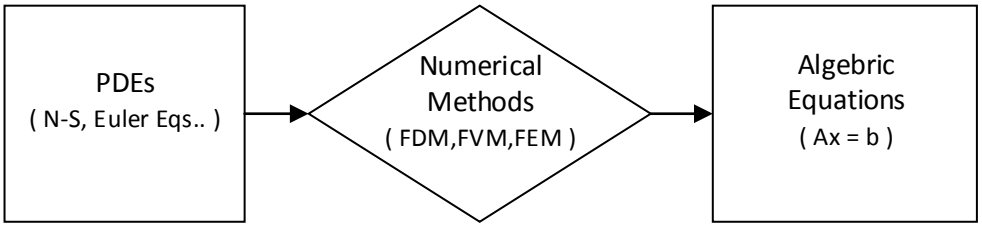

Figure 3.1: CFD objective algorithm summary.

3.1 Numerical Discretization

In this study, a finite-volume method is used, where the governing equations for continuity, momentum, energy and other scalars are used in the integral form. The computational grid provides the discrete control volumes where the integration of the governing equations is performed to form the solution of the problem.

Due to the generally non-linear structure of partial differential equations, they have very few analytical solutions. Therefore it is needed to transform the partial differential equations in both space and time to obtain their algebraic counterparts. The procedure of transforming a partial differential equation into its algebraic or numerical analogue is called numerical discretization. The finite volume method is probably the most popular and widespread approach for numerical discretization. Using the finite volume method the computational space is first divided into a number of non-overlapping control volumes. This is done such that every grid point is surrounded by one control volume. The so-called grid points represent the locations where the flow variables are

actually computed and stored. The conservation equations are then to be written in integral form. The generalized conservation equation for an arbitrary scalar ϕ is:

$$\frac{\partial}{\partial t}\iiint_{\forall}\rho\phi d\forall+\iiint_{\forall}\nabla(\rho u\phi)d\forall=\iiint_{\forall}\nabla(\Gamma\nabla\phi)d\forall+\iiint_{\forall}S_{\phi}d\forall \qquad (3.1)$$

The above equation can be simplified using Gauss' divergence theorem which converts two of the volume integrals in the above equation to surface integrals. Gauss' divergence theorem can be expressed for an arbitrary vector, f as:

$$\iiint_{\forall}\nabla f\, d\forall=\iint_{S}f.\mathbf{n}\, dS \qquad (3.2)$$

where n is the unit vector.

Using Gauss' divergence theorem, volume integrals in a partial differential equation that contain a divergence term are converted to surface integrals, which is needed for spatial discretization. Applying the divergence theorem, equation 4.1 transforms to:

$$\frac{\partial}{\partial t}\iiint_{\forall}(\rho\phi)d\forall+\iint_{S}\mathbf{n}.(\rho u\phi)dS=\iint_{S}\mathbf{n}.(\Gamma\nabla\phi)dS+\iiint_{\forall}S_{\phi}d\forall \qquad (3.3)$$

3.1.1 Conservation Equations

In this project, the conservation of mass, momentum and energy of any scalar Φ for the unsteady flow model can be written as:

$$\frac{\partial\rho\Phi}{\partial t}+\frac{\partial}{\partial x_i}(\rho U_i\Phi-\rho\Gamma_{\Phi}\frac{\partial\Phi}{\partial x_i})=S_{\Phi} \qquad (3.4)$$

Where Γ_{Φ} and S_{Φ} are diffusion coefficient and source term, that should be defined for each equation. The coefficients and terms are given in Fig 3.2 for each scalar:

For example, for continuity equation, $\Phi=1$, $\Gamma_{\Phi}=0$ and $S_{\Phi}=0$ are defined that refers to the mass conservation. There are source terms due to friction and reaction effects associated with Navier-Stokes, enthalpy and species mass fraction equations. The expansion of the polyurethane flow is not expected to be turbulent, but the air flow that is pushed away by polyurethane flow is turbulent. To catch this turbulent flow Unsteady Reynolds Averaged Navier-Stokes (URANS) with $k-\varepsilon$ turbulent model is used. In the process of filling the refrigerator cabinet by rigid polyurethane, the air flow is expected to be turbulent. In the turbulent flow, the velocity and other scalar terms in the N-S

	Φ	Γ_Φ	S_Φ
Continuity	1	0	0
x-mom.	U	$\nu = \frac{\mu}{\rho}$	$-\frac{\partial P}{\partial x_1} + \frac{\partial}{\partial x_i}\left(\mu \frac{\partial U_i}{\partial x_1}\right)$
y-mom.	V	$\nu = \frac{\mu}{\rho}$	$-\frac{\partial P}{\partial x_2} + \frac{\partial}{\partial x_i}\left(\mu \frac{\partial U_i}{\partial x_2}\right)$
z-mom.	W	$\nu = \frac{\mu}{\rho}$	$-\frac{\partial P}{\partial x_3} + \frac{\partial}{\partial x_i}\left(\mu \frac{\partial U_i}{\partial x_3}\right)$
Enthalpy	C_pT	$\frac{\lambda}{\rho C_p}$	$-2\mu\left(\frac{\partial U_i}{\partial x_i}\right)^2 - \mu\left[\left(\frac{\partial U_1}{\partial x_1} + \frac{\partial U_2}{\partial x_2}\right)^2 + \left(\frac{\partial U_1}{\partial x_1} + \frac{\partial U_3}{\partial x_3}\right)^2 + \left(\frac{\partial U_2}{\partial x_2} + \frac{\partial U_3}{\partial x_3}\right)^2\right]$
Mass Fraction	Y_i	D_i	$\dot{S}_i$

Figure 3.2: Diffusion coefficients and source terms [4].

equation includes both a mean and a turbulent component. Reynolds decomposition method basically separates a variable into mean and fluctuating components,

$$u_i = \bar{u}_i + \acute{u}_i \tag{3.5}$$

Where $\bar{u}_i$ represents mean velocity and $\acute{u}_i$ represents the fluctuating components. Likewise, for pressure and any other scalar term:

$$\Phi = \bar{\Phi} + \acute{\Phi} \tag{3.6}$$

Where Φ represents pressure, energy or species mass fraction.

3.1.2 Turbulence Model for Air Phase

In addition to the equation given in the previous section, $k-\varepsilon$ turbulence model which includes wall functions was applied. The effective turbulent stress is:

$$\tau_{T,ji} = \rho(\acute{u}_i\acute{u}_j) = \mu_T\left(\frac{\partial u_j}{\partial x_i}+\frac{\partial u_i}{\partial x_j}\right)-\frac{2}{3}\mu_T\frac{\partial u_l}{\partial x_I}\delta_{ji}-\frac{2}{3}\rho k\delta_{ji} \tag{3.7}$$

Where δ_{ij} is Kronecker's delta:

$$\delta_{ij} = \begin{cases} 1 & \text{if } k=1 \\ 0 & \text{if } k\neq 1 \end{cases} \tag{3.8}$$

and the turbulence viscosity is defined as:

$$\mu_T = \frac{\rho C_\mu k^2}{\varepsilon} \tag{3.9}$$

Where C_μ is constant for standard $k-\varepsilon$ model. $Pr_{T,h}$ is defined as Prandtl number for turbulent flow.

For the reaction species variables, α(in this project, including the mass fraction of isocyanate, polyol, polyurethane, carbamic acid, amine, carbon dioxide, urea, liquid water, vapor, liquid physical blowing, physical blowing vapor) where $\alpha = 1,...12$, the transport equation can be written as:

$$\frac{\partial \rho Y_\alpha}{\partial t}+\frac{\partial \rho u_j Y_\alpha}{\partial x_j} = \frac{\partial}{\partial x_j}(\frac{\mu_T}{Sc_\alpha}\frac{\partial Y\alpha}{\partial x_j})+\rho\bar{Y_\alpha} \tag{3.10}$$

Lewis dimensionless number is assumed to be equal to 1 for all species. Therefore, species mass diffusivity, D_T is constant. Lewis dimensionless number can be represented as follow [19];

$$Le = \frac{Sc}{Pr} \tag{3.11}$$

For α, Sc_α is the dimensionless Schmidt number. All the Schmidt numbers were assumed to be 0.9. Schmidt number (Sc) is a dimensionless number defined as the ratio

of momentum diffusivity (viscosity) and mass diffusivity, and is used to characterize fluid flows in which there are simultaneous momentum and mass diffusion convection processes. The time average of the source terms($\dot{Y}$) should be taken to be applicable in the associated equations. These source terms were abstained from the reaction kinetics analysis code. During the polyurethane injection process in the refrigerator cabinet, air flow has a turbulent structure. Thus $k-\varepsilon$ turbulence model can be implemented in this study.

The realizable k- ε model is a relatively recent development and differs from the standard $k-\varepsilon$ model in two important ways [5]:

•The realizable $k-\varepsilon$ model contains a new formulation for the turbulent viscosity.

•A new transport equation for the dissipation rate, ε, has been derived from an exact equation for the transport of the mean-square vorticity fluctuation.

The modeled transport equations for k and ε in the realizable $k-\varepsilon$ model are

$$\frac{\partial}{\partial t}(\rho k)+\frac{\partial}{\partial x_j}(\rho k u_j)=\frac{\partial}{\partial x_j}\left[\left(\mu+\frac{\mu_t}{\sigma_k}\right)\frac{\partial k}{\partial x_j}\right]+G_k+G_b-\rho\varepsilon-Y_M+S_k \qquad \textbf{(3.12)}$$

$$\begin{aligned}\frac{\partial}{\partial t}(\rho\varepsilon)+\frac{\partial}{\partial x_j}(\rho\varepsilon u_j)&=\frac{\partial}{\partial x_j}\left[\left(\mu+\frac{\mu_t}{\sigma_\varepsilon}\right)\frac{\partial \varepsilon}{\partial x_j}\right]\\&+\rho C_1 S\varepsilon-\rho C_2\frac{\varepsilon^2}{k+\sqrt{\nu\rho}}+C_{l\varepsilon}\frac{\varepsilon}{k}C_{3\varepsilon}G_b+S_\varepsilon\end{aligned} \qquad \textbf{(3.13)}$$

Where

$$C_1=max[0.43,\frac{\eta}{\eta+5}] \qquad \eta=S\frac{k}{\varepsilon} \qquad S=\sqrt{2S_{ij}S_{ij}} \qquad \textbf{(3.14)}$$

In these equations, G_k represents the generation of turbulence kinetic energy due to the mean velocity gradients. G_b is the generation of turbulence kinetic energy due to buoyancy. Y_M represents the contribution of the fluctuating dilatation in compressible turbulence to the overall dissipation rate. C_2 and $C_{1\varepsilon}$ are constants. σ_k and σ_ε are the turbulent Prandtl numbers for k and ε, respectively. S_k and S_ε are user-defined source terms [5].

The eddy viscosity is:

$$\mu_t = \rho C_\mu \frac{K^2}{\varepsilon} \tag{3.15}$$

Where C_μ is no longer constant for k-ε realizable model and it can be solved as [5]:

$$C_\mu = \left(\frac{1}{A_0 + A_s \dfrac{kU^*}{\varepsilon}} \right) \tag{3.16}$$

where

$$U^* \equiv \sqrt{S_{ij}S_{ij} + \tilde{\Omega}_{ij}\tilde{\Omega}_{ij}} \tag{3.17}$$

and

$$\tilde{\Omega}_{ij} = \Omega_{ij} - 2\varepsilon_{ijk}\omega_k \qquad \Omega_{ij} = \overline{\Omega_{ij}} - \varepsilon_{ijk}\omega_k \tag{3.18}$$

where $\overline{\Omega_{ij}}$ is the mean rate-of-rotation tensor viewed in a rotating reference frame with the angular velocity ω_k. The model constants A_0 and A_s are given by:

$$A_0 = 4.04$$

$$A_s = \sqrt{6} cos\phi$$

where

$$\phi = \frac{1}{3}\cos^{-1}(\sqrt{6}W)$$

$$W = \frac{S_{ij}S_{jk}S_{ki}}{\tilde{S}^3}$$

$$\tilde{S} = \sqrt{S_{ij}S_{ij}} \qquad S_{ij} = \frac{1}{2}\left(\frac{\partial u_j}{\partial x_i} + \frac{\partial u_i}{\partial x_j}\right)$$

The model constants are:

$$C_{1\varepsilon} = 1.44,\ C_2 = 1.9,\ \sigma_k = 1.0,\ \sigma_\varepsilon = 1.2$$

3.2 Geometry and Design Parameters

The 3D isometric view of four door refrigerator is shown in Fig 3.3.

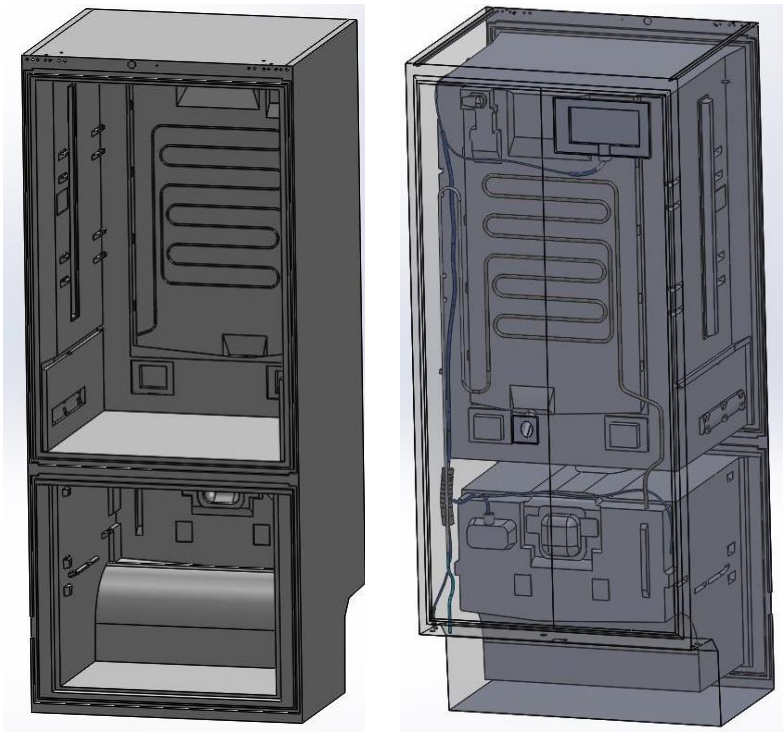

Figure 3.3: Isometric view of refrigerator.

There is a lot of detail in the cabinet. Compressed air channels, electrical cables and evaporator pipe that passed in the back of cabinet are observed. Therefore, the structural complexity will demand a huge grid size for volume that flow is passed through it. The cabinet height is h = 1.43 m, the thickness is d = 0.6 m and the cabinet wide is w = 0.7 m. Fig 3.4 shows the stance of cabinet during the injection process, injection hole and the locations of the air outlet holes. There are 16 holes for air evacuation with one big outlet (Fig 1.2.a) and 15 small holes.

The biggest outlet hole that is located at the top face of the cabinet has a diameter of 19 mm, the smallest outlet hole that is shown in the right hand side of the biggest one has a diameter of 3.2 mm and the diameters of the other holes is 6 mm as shown in

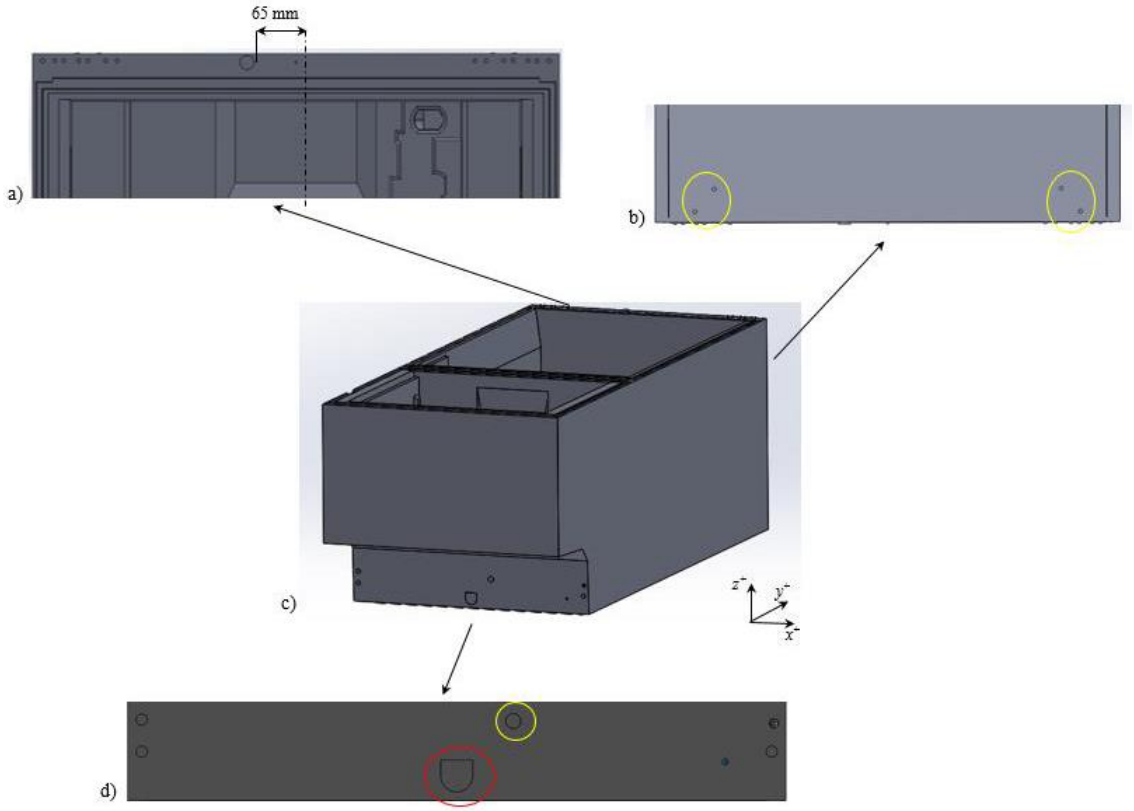

Figure 3.4: Cabin's position during the injection process.

Fig3.4. The electrical cables holes that are enclosed in the yellow circles are shown at the top of the refrigerator (Fig 1.2.b). The cabinet is laid back during the polyurethane injection process (Fig 1.2.c). The material will be injected into the cabinet cavity from the inlet hole with about 53.4 mm diameter as shown enclosed with a red circle and just above this hole, there is another air inlet hole with diameter of 16 mm that is enclosed with a yellow circle (Fig 1.2.d).

3.3 Grid Generation

Computational fluid dynamics (CFD) simulations require the computational domain to be discretized into cells so that in each cell, transported quantities are solved with continuity, momentum and energy equations. Therefore, meshing is one of the most important steps of a CFD simulation process. Grid generation for complex geometries is usually a difficult task witch is both money and time consuming. In the present work, computational grid of the geometry was created using a commercial software. The two traditional approaches are: structured body-fitted mesh from multi-block structure, in which the blocks may overlap and the use of a completely unstructured body-fitted mesh. Both of this methods need significant efforts in grid generation in the aspect of the body-fitting and accuracy which need much more time to generate fine mesh for CFD analysis. By considering these restrictions, Cartesian cut cell meshing approach could be a great solution [20]. At surfaces, the cells can be locally refined to better model the geometry and flow [21].

Cartesian CFD methods have several advantages over methods that use a body fitted mesh. Firstly, the meshing process is considerably more straightforward and easily automated and hence the time taken to mesh a complex geometry is significantly low. Secondly, the finite volume flow equations are simpler as the mass flux through each face depends on only one velocity component rather than all components and finally, the additional computational effort involved in problems with moving boundaries is greatly reduced because, after each time step, only the cells adjacent to the moving boundary need to be adapted rather than the whole mesh [22].

3.4 The Cartesian Cut Cell Method

The CutCell mesher converts a volume mesh into a mainly Cartesian mesh which consists of mostly hexahedral elements, with faces that are aligned with the coordinates axes. Using smaller element will help to resolve details of the complex geometry, and the interfaces between the different size elements are non-conformal as shown in the Fig 3.5.

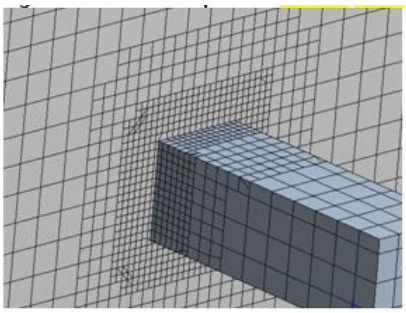

Figure 3.5: Cut cell mesh with different size element at the interface.

Cut Cell meshing method was used to generate CFD simulation grids by using ANSYS Meshing software for refrigerator cabinet. By the usage of these meshing method, CFD analysis has become more easier task for refrigerator complex geometry.

Fig 3.6 shows the generated mesh for cabinet cavity. Electric Cable inside the cabinet, evaporation pipes and other structural details Fig 3.7 have increased the number of cells that were needed for the flow analysis. Therefore, in the narrow and complex channel, turbulent, reactive and two-phase flow could be investigated very close to the reality. 3.4 million cells were generated using Ansys cutcell meshing method.

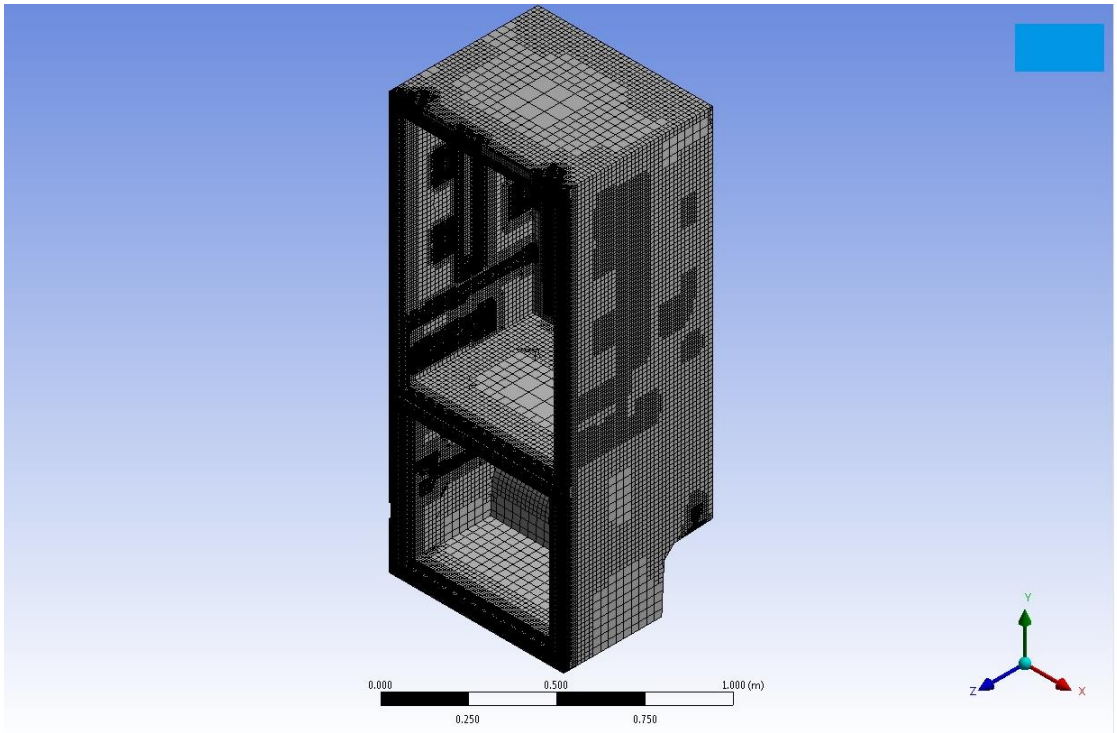

Figure 3.6: Isometric view of cabinet mesh.

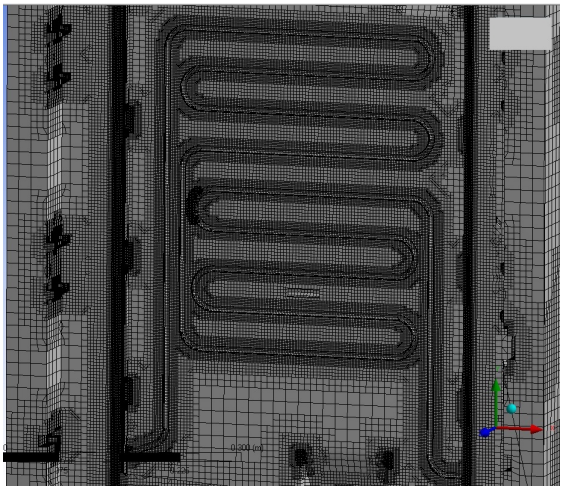

Figure 3.7: Isometric view of cabinet mesh.

Generated mesh around the air outlet holes and injection hole are shown in Fig 3.8 and Fig3.9 respectively. The mesh size is more tight into the holes and it is going to be more sparse gradually moved away from the hole. By this way, the complex turbulent flow in the area close to the holes is solved more accurately.

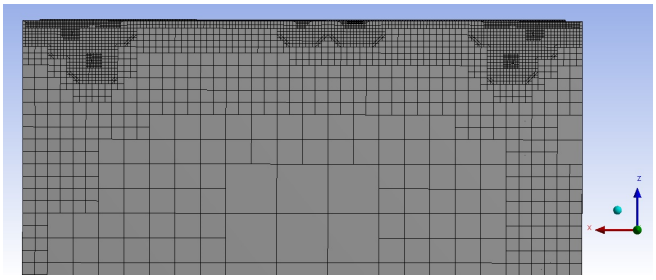

Figure 3.8: Generated mesh around the holes.

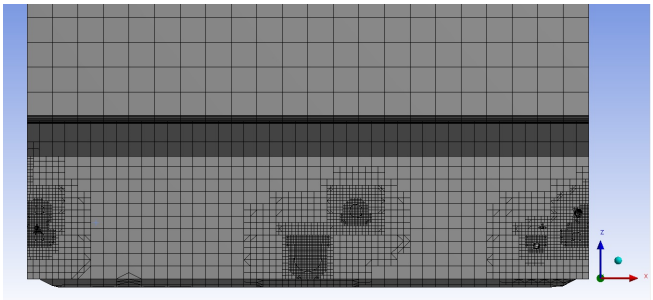

Figure 3.9: Generated Mesh around the holes.

The refrigerator should be kept in the laid back position during the polyurethane injection process. The stance position during, injection and outlet holes are shown in Fig 3.10.

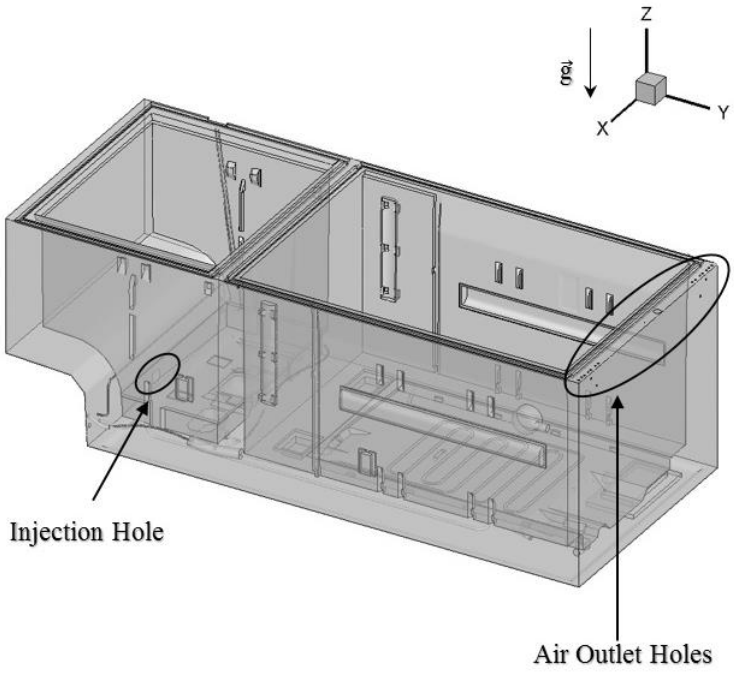

Figure 3.10: Cabin stance during the injection.

This is the stance position of the cabinet in the CFD calculations and injection hole is positioned to the symmetry on X axis of the cabinet.

3.5 The CFD Solver

In this study, Operation conditions for the real injection process were applied one by one to CFD analysis. After compatibility testing of the CFD results with actual process results, several suggestions have been made for possible improvements. FLUENT 6.3 software was used for CFD analysis. The Reaction kinetics modeled separately and then it was imported into the CFD software to model reactive flow. These process are provided by User Defined Functions (UDFs) in the CFD software. UDF is used to take properties of flow in the FLUENT solver to more advanced level. For example using a UDF can help to define user's own boundary conditions, material properties and source terms for flow region, define models with different parameters (e.g., multiphase model), postproseccing enhancement, initialize a solution and etc [5]. UDFs are written in the C programming language. In this study, UDFs are used for 11 species and produced mixture to calculated density, viscosity, enthalpy and temperature, diffusions, the reactions and phase changes. The pressure based segregated algorithm which

is based on solving momentum equations first and then correcting it to satisfy the continuity equation, is used. This is an iterative algorithm where solved velocity field is updated by the conservation of mass constantly. When the segregated method is used, it means that the velocity equations are solved separately as well as the other equations. The pressure-based algorithm can be shown as Fig 3.11.

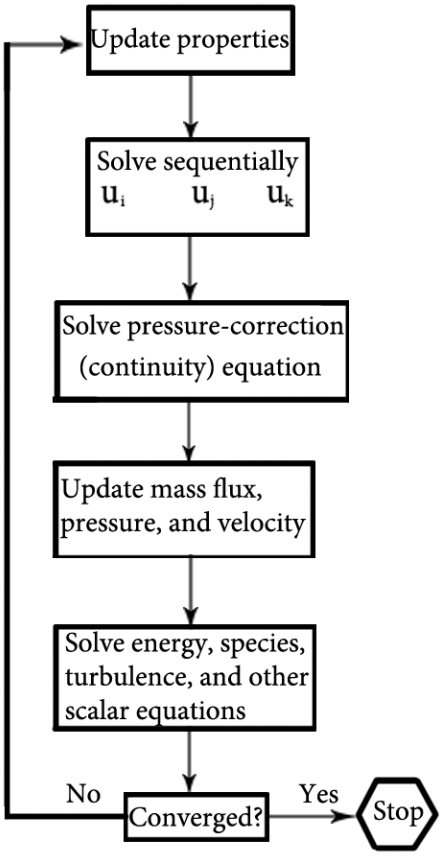

Figure 3.11: Pressure based segregated algorithm summary [5].

FLUENT provides three methods for pressure-velocity coupling in the segregated solver: SIMPLE, SIMPLEC, and PISO. Steady-state calculations will generally use SIMPLE or SIMPLEC, while PISO is recommended for transient calculations. PISO may also be useful for steady state and transient calculations on highly skewed meshes [5]. The Pressure-Implicit with Splitting of Operators (PISO) pressure-velocity coupling scheme, part of the SIMPLE family of algorithms, is based on the higher degree of the approximate relation between the corrections for pressure and velocity. One of the limitations of the SIMPLE and SIMPLEC algorithms is that new velocities and corresponding fluxes do not satisfy the momentum balance after the pressure-correction equation is solved. As a result, the calculation must be repeated

until the balance is satisfied. To improve the efficiency of this calculation, the PISO algorithm performs two additional corrections: neighbor correction and skewness correction.

The main idea of the PISO algorithm is to move the repeated calculations required by SIMPLE and SIMPLEC inside the solution stage of the pressure-correction equation. After one or more additional PISO loops, the corrected velocities satisfy the continuity and momentum equations more closely. This iterative process is called a momentum correction or "neighbor correction". The PISO algorithm takes a little more CPU time per solver iteration, but it can dramatically decrease the number of iterations required for convergence, especially for transient problems.

For meshes with some degree of skewness, the approximate relationship between the correction of mass flux at the cell face and the difference of the pressure corrections at the adjacent cells is very rough. Since the components of the pressure-correction gradient along the cell faces are not known in advance, an iterative process similar to the PISO neighbor correction described above is desirable. After the initial solution of the pressure-correction equation, the pressure-correction gradient is recalculated and used to update the mass flux corrections. This process, which is referred to as "skewness correction", significantly reduces convergence difficulties associated with highly distorted meshes. The PISO skewness correction allows FLUENT to obtain a solution on a highly skewed mesh in approximately the same number of iterations as required for a more orthogonal mesh. Neumann boundary condition was applied to scalars in the air outlet hole At the walls, zero-flux boundary condition will be used for scalars.

3.6 User Defined Function

A user-defined function or in short UDF is a C based program that is written separately for the CFD code to specify special features to the standard program. For example, UDFs can be written to define different boundary conditions, material properties, source terms or model properties for the specific problem. This way, the code can be customized according to the problem to be solved and an enhancement in the solution quality overall can be achieved. In this thesis, the enthalpy equation was solved using a UDF. In the UDF used, enthalpy was defined as a user-defined scalar (UDS) and solved using transport equation. Some of the most important features and macros used by UDFs that are also included in the UDF written for the present simulation will be explained below.

Define Profile

Define profile macro in UDF defines a custom boundary profile function that is dependent on space or time, in other words it can be used to define special boundary conditions. Temperature, velocity, pressure, turbulence kinetic energy, turbulence dissipation rate etc. are some examples of variables that was specified at the boundaries by Define Profile. In the UDF used for the present simulations, profiles were written to define inlet enthalpy and outlet back flow enthalpy.

Define Adjust

Define adjust is a general purpose macro that can be used to modify flow variables like pressure, velocity etc. or compute integrals of scalar quantities and adjust boundary conditions accordingly. The most important feature of define adjust is that, it executes at the beginning of every iteration regardless of the solution being time dependent or independent. Define adjust macro is called before transport equations are solved. In this thesis, define adjust macro was used for obtaining temperatures from enthalpy values.

Define Execute at End

Execute at end is another general purpose macro that differs from define adjust with the way it is executed. Different from define adjust, it is executed at the end of every iteration for a steady state calculation and executed at the end of every time step for an unsteady calculation. The execution is done automatically when the solution method is chosen. Define adjust and execute at end are especially important to build the numerical algorithm of the calculation. In the UDF used for the present simulations, boundary temperature calculations and temperature modifications were performed at every time step using execute at end command.

Define Execute on Loading

"Execute on loading" is used when it is needed to initialize or set-up UDF models when a UDF library is loaded. It is a general purpose macro with the characteristic to execute right after the UDF library is loaded. Also it is useful to reserve user defined scalars (UDS) or user defined memories (UDM) for a particular library. In this thesis, in execute on loading macro, some global variables, model constants etc. were specified as well as boundary ID assignments.

Define Property

Define property is used to specify a custom material property in the code. Using define property macro, properties such as density, viscosity, thermal conductivity etc. can be designated. In this study, define property macro was used to define mixture density of air and also to calculate laminar viscosity.

Define Init

Define init is used to specify initial values for the solution. This macro is executed once for every initialization and is called after solver initialization. In this problem, inlet density, inlet enthalpy and inlet temperature were assigned using define init macro.

Define Diffusivity

Define diffusivity is used when it is needed to specify the turbulent diffusivity for transport equations or UDS transport equations. In this study define diffusivity was used to specify turbulent diffusivity of the enthalpy equation.

User Defined Scalars-UDSs

User defined scalars are used when it is needed to solve transport equations for additional scalars. Defined UDSs are solved the same way the scalars are solved. The general transport equation that is used for an arbitrary scalar ϕ is defined as:

$$\iiint_{\forall} \frac{\partial \rho \phi}{\partial t} d\forall + \iint_{S} \rho \phi \mathbf{u} dS = \iint_{S} \Gamma_{\phi} \nabla \phi dS + \iiint_{\forall} S_{\phi} d\forall \qquad (\mathbf{3.19})$$

where Γ_{ϕ} is the diffusion coefficient for ϕ and S_{ϕ} is the source term for ϕ . The enthalpy equation was solved for the present simulations using a user defined scalar.

User Defined Memory (UDM)

If it is required to store some variables and use them in the process or post process, user defined memory (UDM) could be used. In this study, temperature values are needed for post processing and also for backup reasons, pressure values were also stored, therefore the number of UDMs used was two.

UDF Process for Pressure Based Segregated Solver

For the pressure based segregated algorithm, the solution procedure for UDFs start with the general initialization. After that, initialization that is defined in the UDF is called. This process overwrites the previous general initialization. After initialization, the variables that are defined as profiles are called which describes boundary values as mentioned before. The solution iterations begin with functions that are defined in adjust macros. Following, momentum equation for velocity components are solved. Sequentially continuity equation is solved and velocity is updated accordingly. Consequently, the energy and species equations; and turbulence and other transport equations are solved.

The boundary and initial conditions for CFD analysis that are given by the manufacturer are shown as Table 3.1. The mixture of species with pre-specified mass fractions is injected to the refrigerator cabinet with 1.5 kg/s mass flow rate over 4.47 seconds. The initial temperature for species is 21 °C, but during the actual injection process the wall of the cabinet is heated up to 40 °C, before injection. The effect of temperature on the reaction speed was mentioned in the previous section. Therefore,

Table 3.1: Initial conditions

T_{cabin}	313.15 K
$Y_{isocyanate}$	0.57
Y_{water}	0.0095
Y_{polyol}	0.3705
Y_{PBA}	0.05
$t_{injection}$	4.47 [s]
$\dot{m}$	1.5 kg/s
P_{out}	1 atm

a faster reaction is expected in the material to wall (refrigerator cabinet) contact zone. The mole fraction of the species in the injected mixture is represented in Table 3.1.

There are 8 species and physical blowing agent in liquid and vapor phase, liquid water and its vapor. Therefore, transport equation should be solved for 11 parameters. The reactions occur with initial values such as initial temperature and species initial mass fractions. At the end of the reactions, new temperature and mass fractions are calculated then they are sent back to the CFD software. The calculation of the source term is done by subtracting new temperature and mass fraction from old values and dividing them by time step. This source term is added to the CFD calculations in the next time step as follow:

1. Model and refine the 3 dimensional geometry of the refrigerator cabinet.

2. Apply mesh generation to divide volume in to the small cells for the CFD analysis.

3. Import CFD and Reaction Kinetics models based on initial and boundary conditions.

4. Implement initial conditions ($T_{initial}$, $Y_{i_{initial}}$, P).

5. Implement CFD analysis to solve momentum, continuity and energy conservation equations using $k-\varepsilon$ model for time step Δt ($t_{new} - t_{old} = \Delta t$).

6. Do calculation until the solution is converged if not go to step 5.

7. Get output values for temperature (T_{output}) and species mass fraction ($Y_{i_{output}}$) from the CFD calculations.

8. Implement T_{output} and $Y_{i_{output}}$ in the reaction kinetics calculations.

9. Get new values for temperature (T_{new}) and species mass fraction ($Y_{i_{new}}$) from the reaction kinetics calculations.

10. Calculate the source term for the species, enthalpy and phase change.

11. Evaluate the results and go to step 5.

4. RESULTS and DISCUSSIONS

According to the previous chapters:

•Finite volume method (FVM) has been used for CFD analysis while mesh generation has been don using cutcell meshing method.

•The equations of mass, momentum (3d) and energy (enthalpy) conservation has been solved.

•The air that is pushed away from the refrigerator cabinet is turbulent. Therefore, $k-\varepsilon$ URANS turbulence model has been applied.

•The total number of species that should be transported is S_T, while there are S species in the reaction mixture(S=8), and other three are physical blowing agent and its vapor and vapor of water.

$$S_T = S + 3 = 11$$

•If the value of density is high, the time step was brought down to 1×10^{-4} s. But generally, it is 0.05 s, and the maximum value for time step is 1 s.

4.1 Results

In Fig 1.3, polyurethane reaction process was divided into several steps. From these stages, the gel time is related to the reaction of methyl diisocyanate (MDI) and polyol, tack-free time is associated with the formation of urea. By considering the modeling of chemical reactions using this approach, the gelling process associated with formation of polyurethane begin at the first stages and urea is expected to have slow formation and starts later. The concentration of polyurethane and urea are very important in this study because they are related to gelling and blowing reactions which play a big role in polyurethane foam injection with solidification process. Other intermediate species which are being produced and consumed during the process have less impact,

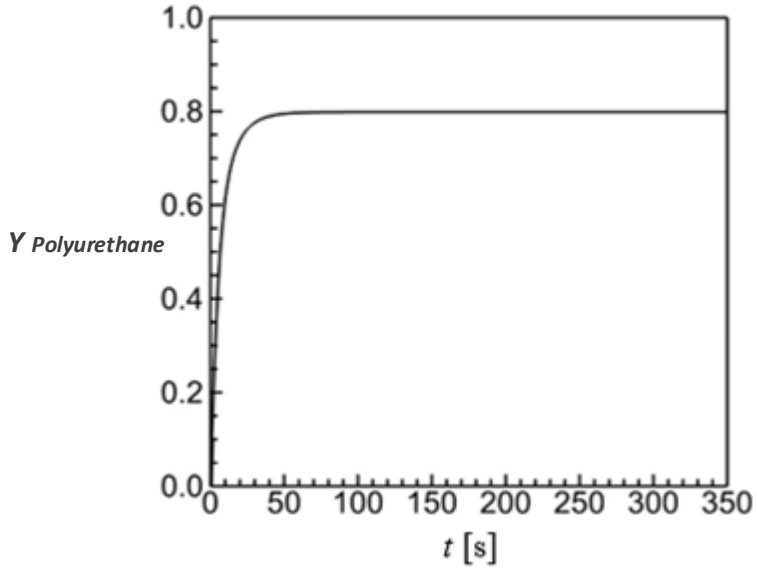

Figure 4.1: Polyurethane Mass Fraction versus time.

while polyurethane and urea are important and determine the physical properties of polyurethane foam at the end of reactions. Fig 4.1 represents the polyurethane mass fraction versus time. It is observed that polyurethane's production occurs rapidly in the first 50 seconds of the reaction, then the concentration did not change much more.

Fig 4.2 represents the variation of mass fraction of urea as a function of time, which is calculated using reaction kinetics model. The comparison of the formation of urea to polyurethane shows that, the production of urea seems to occur slowly rather than polyurethane's production as it expected from Fig 1.3 where Tack-free time occurs at 40-75 seconds. The mass fraction of urea has reached a values of 0.1180 at the end of 350 seconds. The curve seems to not to increase between the range of 100-350 seconds.

Fig 4.3 represents the temperature variation over the time which is calculated using reaction kinetics model, where the temperature curve shows a good similarity to the generated temperature curve with the experimental data shown in Fig 1.3. Temperature increases rapidly and reaches to about 160 °Cat the end of 350 seconds. The curve formed by the reaction kinetics model shows a slightly sharp rise compared to experimental data.

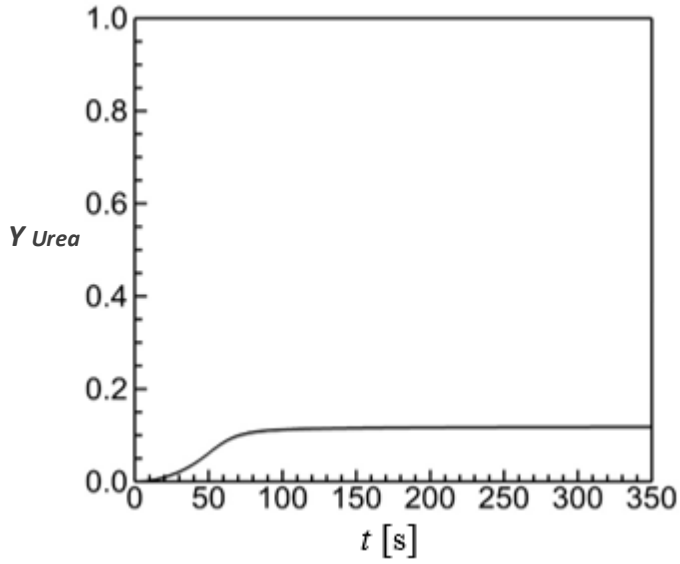

Figure 4.2: Urea Mass Fraction versus time.

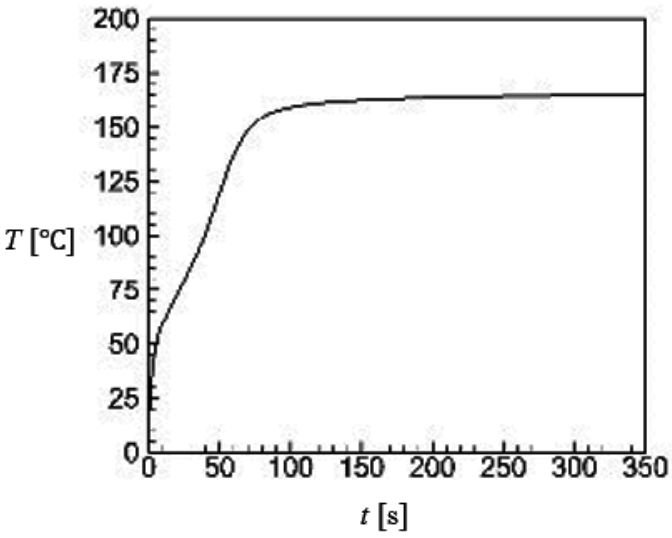

Figure 4.3: Temperature variation versus time.

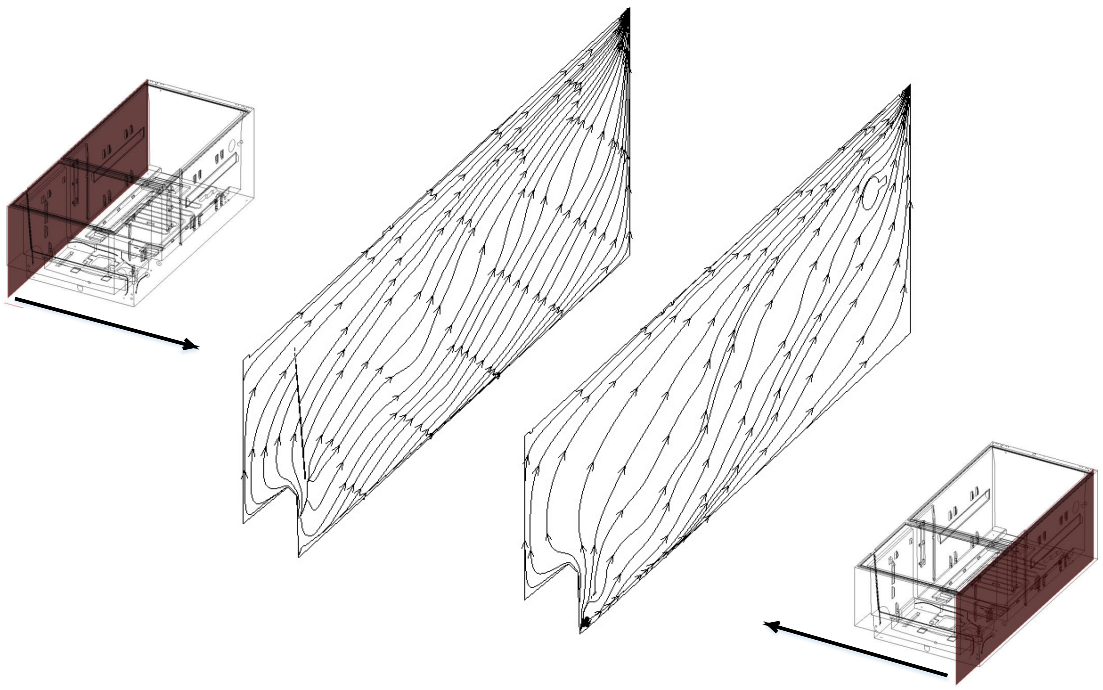

Figure 4.4: Streamline distributions.

The $K-\varepsilon$ method which models every scale of turbulence in the flow field. The streamlines pattern is shown in Fig 4.4 for cabinet's left and right hand sides planes. It is observed that, the flow streamlines have parallel structure at the zone far from outlet holes, but they come closer at the zone close to outlet holes which indicates that all the streamline are directed toward the outlet holes. Fig 4.5 and Fig 4.6 represents the streamlines distribution for cabinet's top and middle plane respectively. There is no reverse flow at outlets which means that the flow is well established. The diameter of outlet has a big impact on flow streamlines. The big part of the flow tends to go out from the hole with biggest diameter.

The distribution of mass fraction of polyurethane at the end of the process is shown in Fig 4.7. As it mentioned in Fig 2.1, polyurethane is the product of isocyanate and polyol reaction which is known as the gelling reaction. Polyurethane is produced in the reaction zone close to injection area, then it transported gradually to the upper zones of the cabinet, but not fully filled the potentially problematic zones.

Fig 4.8 represents the mass fraction of urea at the end of process. As it mentioned in Fig 2.1, urea is produced in the isocyanate and amine reaction. It should be noted that urea production starts at the last seconds of the process and continues for a long time.

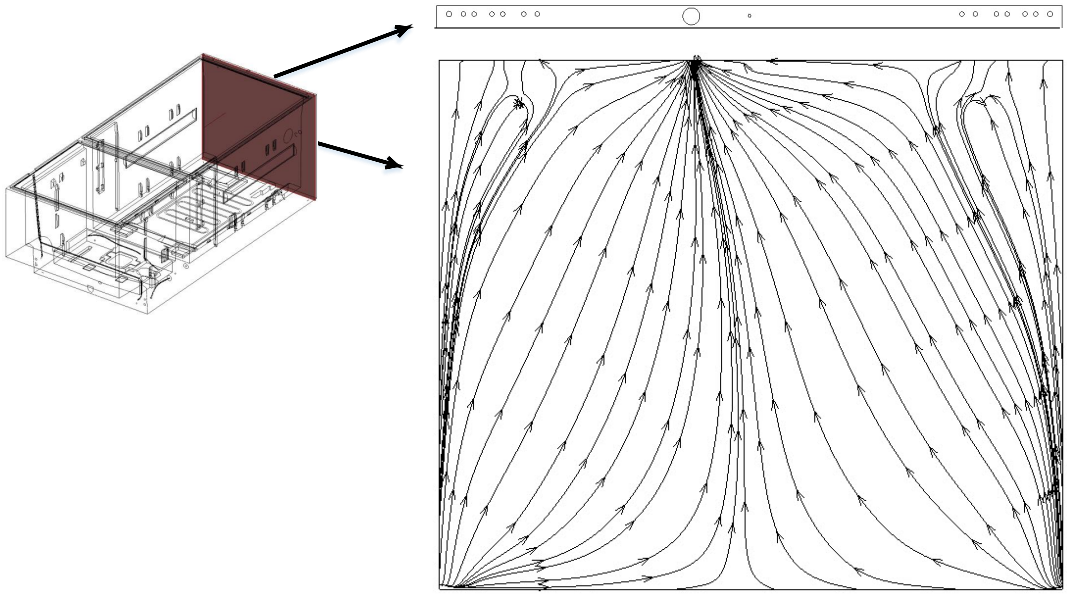

Figure 4.5: Streamline distributions.

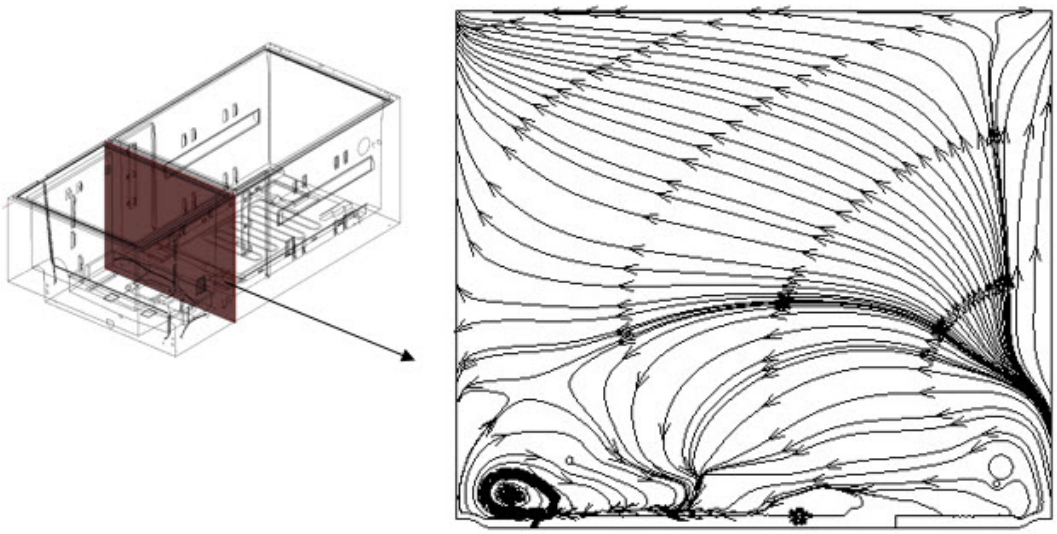

Figure 4.6: Streamline distributions.

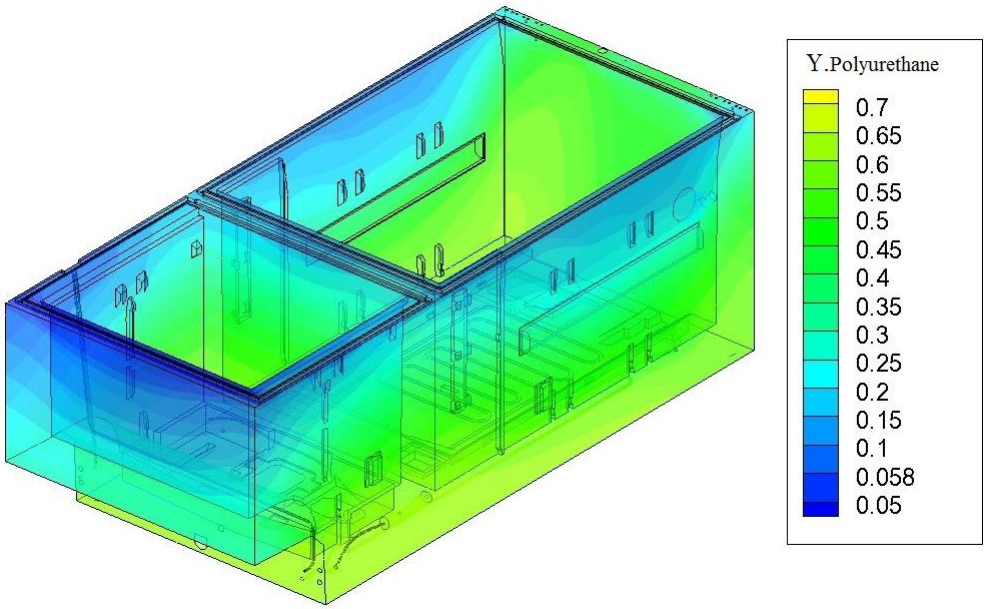

Figure 4.7: Polyurethane mass fraction.

Therefore, much longer periods of time is required for simulations to observe the latest state of the urea concentration.

Figure 4.9 Simulation results shows the polyurethane foam flow on the molding filling time. According to Fig 5.8.1 thick cables and various cabinet components in front of the injection hole are seen that change foam flow direction left hand side which has less geometrical complexity. Fig 5.8.2 shows much more expansion of foam toward straight, left and right side and the effect of geometrical complexity on the foam flow path is visible here. Fig 5.8.3 shows the upward expansion of foam into the channel that is located at the middle of the cabinet. The reason of this expansion could be the resistance of the foam flow caused by the evaporation channels and expansion as the result of a chemical reaction. Fig 5.8.4 shows the expansion of the foam in the cabinet right-hand side while there is a continuous upward expansion in the middle channel. Fig 5.8.5 indicates the flow resistance and pressure drop as the result of surface irregularity and geometrical complexity has caused the flow to be amassed in the middle of the cabinet, but the flow overcomes its resistance and covers all over the evaporation channels. According to Fig 5.8.6, although there is a continues flow progress in the middle of cabinet, it is seen that the actual extent of foam flow is at the right and left sides.

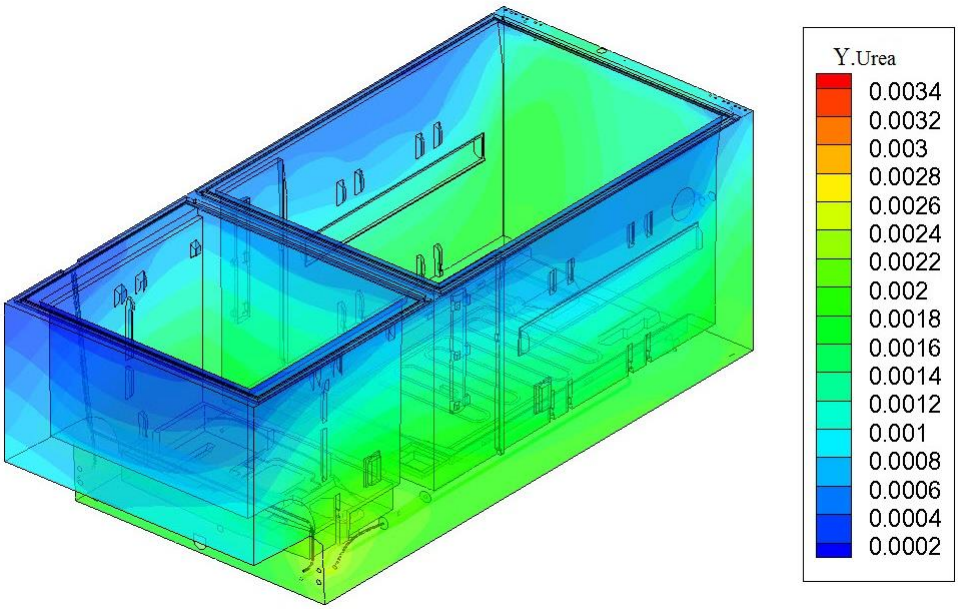

Figure 4.8: Urea mass fraction.

Fig 5.8.7 shows that the flow reaches to the last channel and extends toward the outlet holes. More foam progress at the left side of the cabinet is observed. It is believed that more expansion of the foam in the left side is due to the biggest air outlet hole that is located a little left far from to the symmetric line of the cabinet in the X direction. The foam flow tends to progress toward the hole which has the biggest diameter that is clear in Fig 5.8.8. Moreover, it is shown that the flow expands to outlet holes from the right and left side and has less expansion at the middle part of the cabinet due to flow resistance and pressure drop as a result of surface irregularity and geometrical complexity. In the Fig 5.8.9 the flow has reached to the holes completely, but it has not fully filled the left, right and injection side of the cabinet. Therefore, it can be said that the polyurethane foam flow reached the outlet holes and went out without fully filling the cabinet volume. 5.8.10 shows that the foam expansion continues and the empty spaces which can be called problematic zones are going to be filled slowly. According to the Fig 5.8.11 cabinet zones close to outlet holes fully filled. The empty zone above the injection hole is filling very slow. Foam flow was almost stopped and the empty zone above the injection hole which can be seen in Fig 5.8.12. This zone is known as the problematic zone because lack of polyurethane foam there mean lack of insulation material which will cause to law energy efficiency.

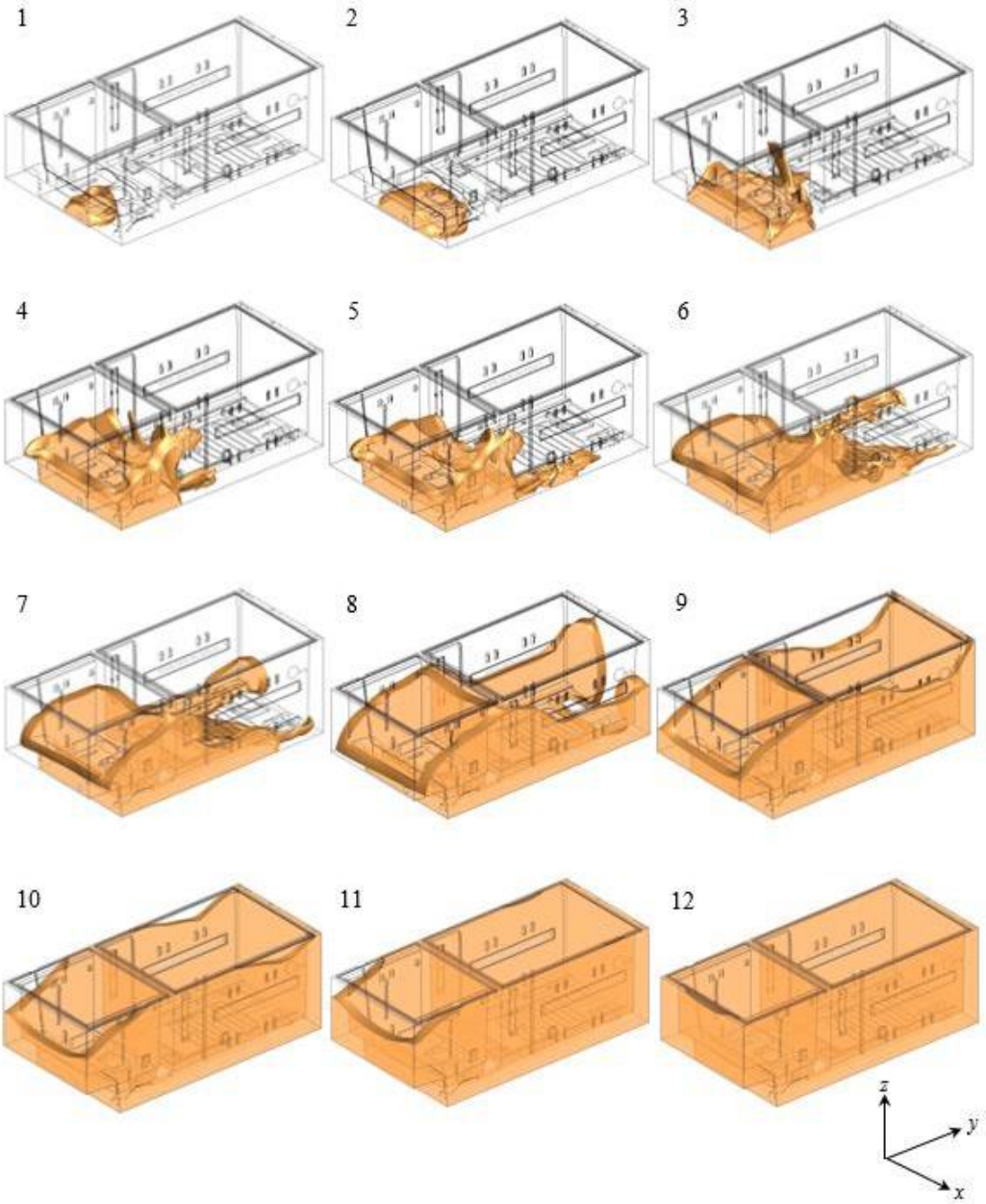

Figure 4.9: Polyurethane foam flow on the 2 door refrigerator cabinet.

4.2 Discussion

To obtain a continuous foam expansion in the refrigerator cabinet especially above the evaporator channels, it is recommended to create special foam flow paths to allow the foam to cover the geometry completely. This zone is sorrounded by blue circle that is shown in Fig 4.10.a.

To evacuate the trapped air in the potentially problematic zones surrounded by blue curves and accelerate the foam expansion Fig 4.10, it is recommended to open new air outlet holes.

According to the CFD simulation results, the zone above the injection hole surrounded by the red curve is not fully filled with foam Fig 4.10.b. Therefore, it is recommended to open new air outlet hole to overcome this problem.

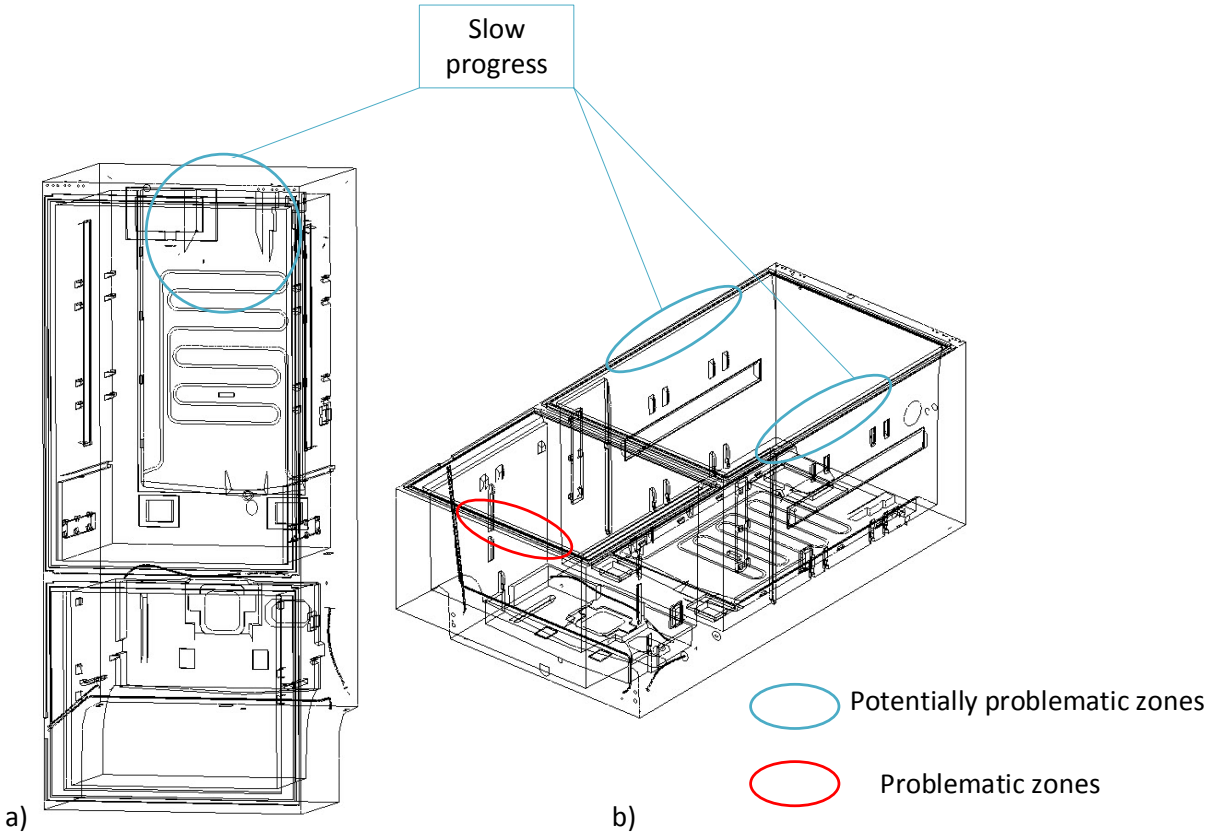

Figure 4.10: Potentially problematic zones in polyurethane injection process.

REFERENCES

[1] **Szycher, M.**, 1999. Szycher's handbook of polyurethanes, CRC press.

[2] **Randall, D. and Lee, S.**, 2002. The polyurethanes book, Huntsman Polyurethanes Belgium.

[3] **Herrington, R. and Hock, K.**, 1998. Flexible polyurethane foams Dow Chemical Co, *Midland, MI*.

[4] **Anderson, D.A.**, **Tannehill, J.C. and Pletcher, R.H.**, 1984. Computational fluid dynamics and heat transfer, *MacGraw-Hill Book Company*.

[5] **Fluent, I.**, 2006. Fluent 6.3 Users Guide, *Fluent documentation*.

[6] **Samkhaniani, N.**, **Gharehbaghi, A. and Ahmadi, Z.**, 2013. Numerical simulation of reaction injection molding with polyurethane foam, *Journal of Cellular Plastics*, **49(5)**, 405–421.

[7] **Baser, S. and Khakhar, D.**, 1994. Modeling of the Dynamics of Water and R-11 blown polyurethane foam formation, *Polymer Engineering & Science*, **34(8)**, 642–649.

[8] **Kim, Y.B.**, **Do Kim, K.**, **Hong, S.E.**, **Kim, J.G.**, **Park, M.H.**, **Kim, J.H. and Kweon, J.K.**, 2005. Numerical simulation of PU foaming flow in a refrigerator cabinet, *Journal of cellular plastics*, **41(3)**, 251–266.

[9] **Seo, D. and Youn, J.R.**, 2005. Numerical analysis on reaction injection molding of polyurethane foam by using a finite volume method, *Polymer*, **46(17)**, 6482–6493.

[10] **Mitani, T. and Hamada, H.**, 2003. Prediction of flow patterns in the polyurethane foaming process by numerical simulation considering foam expansion, *Polymer Engineering & Science*, **43(9)**, 1603–1612.

[11] **Chung, M.H.**, 2006. Cartesian cut cell approach for simulating incompressible flows with rigid bodies of arbitrary shape, *Computers & Fluids*, **35(6)**, 607–623.

[12] **Url-3**, `http://www.nogrid.com/index.php/en/`, date retrieved : 18.04.2015.

[13] **Geier, S.**, **Winkler, C. and Piesche, M.**, 2009. Numerical simulation of mold filling processes with polyurethane foams, *Chemical Engineering & Technology*, **32(9)**, 1438–1447.

[14] **Ni, H.**, **Nash, H.A.**, **Worden, J.G. and Soucek, M.D.**, 2002. Effect of catalysts on the reaction of an aliphatic isocyanate and water, *Journal of Polymer Science Part A: Polymer Chemistry*, **40(11)**, 1677–1688.

[15] **Url-1**, `http://haltermann.com/`, date retrieved : 18.04.2015.

[16] **Turner, S.**, 1972, An introduction to combustion, concepts and applications.

[17] **Warnats, J.**, **Maas, U. and Dibble, R.**, 2000. Combustion, *Physical and Chemical Fundamentals, Modeling and Simulation, Experiments, Pollutant Formation*.

[18] **Munson, B.R.**, **Rothmayer, A.P. and Okiishi, T.H.**, 2012. Fundamentals of fluid mechanics, Wiley Global Education.

[19] **Derbentli, T.**, **Genceli, O.**, **Güngör, A.**, **Hepbaşlı, A.**, **İlken, Z.**, **Özbalta, N.**, **Özgüç, F.**, **Parmaksızoğlu, C. and Urakan, Y.**, 2001. Isı ve Kütle Geçişinin Temelleri, *Literatür Yayıncılık, Dördüncü Basımdan Çeviri, İstanbul*.

[20] **Ingram, D.M.**, **Causon, D.M. and Mingham, C.G.**, 2003. Developments in Cartesian cut cell methods, *Mathematics and Computers in Simulation*, **61(3)**, 561–572.

[21] **Tucker, P. and Pan, Z.**, 2000. A Cartesian cut cell method for incompressible viscous flow, *Applied Mathematical Modelling*, **24(8)**, 591–606.

[22] **Johnson, M.W.**, 2013. A novel Cartesian CFD cut cell approach, *Computers & Fluids*, **79**, 105–119.

CURRICULUM VITAE

Name Surname: Hamed Pahlavani

Place and Date of Birth: Iran, 1988

Adress: Hacı Osman Bayırı Cac. PTT Evleri Mahalesi NO:20. İstanbul

E-Mail: pahlavanihamed@itu.edu.tr

B.Sc.: Azad University of Khoy, Mechanical Engineering Department

M.Sc.: Istanbul Technical University, Mechanical Engineering Department

Scholarships: SAN-TEZ Scholarship